Permeant calcium ion feed-through regulation of single inositol 1,4,5-trisphosphate receptor channel gating

Horia Vais,[1] J. Kevin Foskett,[1,2] Ghanim Ullah,[3] John E. Pearson,[3] and Don-On Daniel Mak[1]

[1]Department of Physiology and [2]Department of Cell and Developmental Biology, Perelman School of Medicine, University of Pennsylvania, Philadelphia, PA 19104

[3]Theoretical Biology and Biophysics, T-6 MS K710, Los Alamos National Laboratory, Los Alamos, NM 87545

The ubiquitous inositol 1,4,5-trisphosphate ($InsP_3$) receptor ($InsP_3R$) Ca^{2+} release channel plays a central role in the generation and modulation of intracellular Ca^{2+} signals, and is intricately regulated by multiple mechanisms including cytoplasmic ligand ($InsP_3$, free Ca^{2+}, free ATP^{4-}) binding, posttranslational modifications, and interactions with cytoplasmic and endoplasmic reticulum (ER) luminal proteins. However, regulation of $InsP_3R$ channel activity by free Ca^{2+} in the ER lumen ($[Ca^{2+}]_{ER}$) remains poorly understood because of limitations of Ca^{2+} flux measurements and imaging techniques. Here, we used nuclear patch-clamp experiments in excised luminal-side-out configuration with perfusion solution exchange to study the effects of $[Ca^{2+}]_{ER}$ on homotetrameric rat type 3 $InsP_3R$ channel activity. In optimal $[Ca^{2+}]_i$ and subsaturating $[InsP_3]$, jumps of $[Ca^{2+}]_{ER}$ from 70 nM to 300 µM reduced channel activity significantly. This inhibition was abrogated by saturating $InsP_3$ but restored when $[Ca^{2+}]_{ER}$ was raised to 1.1 mM. In suboptimal $[Ca^{2+}]_i$, jumps of $[Ca^{2+}]_{ER}$ (70 nM to 300 µM) enhanced channel activity. Thus, $[Ca^{2+}]_{ER}$ effects on channel activity exhibited a biphasic dependence on $[Ca^{2+}]_i$. In addition, the effect of high $[Ca^{2+}]_{ER}$ was attenuated when a voltage was applied to oppose Ca^{2+} flux through the channel. These observations can be accounted for by Ca^{2+} flux driven through the open $InsP_3R$ channel by $[Ca^{2+}]_{ER}$, raising local $[Ca^{2+}]_i$ around the channel to regulate its activity through its cytoplasmic regulatory Ca^{2+}-binding sites. Importantly, $[Ca^{2+}]_{ER}$ regulation of $InsP_3R$ channel activity depended on cytoplasmic Ca^{2+}-buffering conditions: it was more pronounced when $[Ca^{2+}]_i$ was weakly buffered but completely abolished in strong Ca^{2+}-buffering conditions. With strong cytoplasmic buffering and Ca^{2+} flux sufficiently reduced by applied voltage, both activation and inhibition of $InsP_3R$ channel gating by physiological levels of $[Ca^{2+}]_{ER}$ were completely abolished. Collectively, these results rule out Ca^{2+} regulation of channel activity by direct binding to the luminal aspect of the channel.

The Journal of General Physiology

INTRODUCTION

Modulating cytoplasmic free Ca^{2+} concentration ($[Ca^{2+}]_i$) is a universal intracellular signaling pathway that regulates numerous cellular physiological processes including apoptosis, gene expression, bioenergetics, secretion, immune responses, fertilization, muscle contraction, and synaptic transmission (Clapham, 1995; Marks, 1997; Berridge, 1998, 2003; Berridge et al., 2000; Bootman et al., 2001; Orrenius et al., 2003; Braet et al., 2004; Randriamampita and Trautmann, 2004; Cárdenas et al., 2010). Ubiquitous ER-localized inositol 1,4,5-trisphosphate ($InsP_3$) receptor ($InsP_3R$) Ca^{2+} release channels (Foskett et al., 2007) play a central role in this pathway in many cells (Taylor and Richardson, 1991; Putney and Bird, 1993; Bezprozvanny and Ehrlich, 1995; Furuichi and Mikoshiba, 1995; Patterson et al., 2004; Foskett et al., 2007; Joseph and Hajnóczky, 2007; Cárdenas et al., 2010; Foskett, 2010). $InsP_3$ generated in the cytoplasm in response to extracellular stimuli (Berridge, 1993) binds to and activates $InsP_3R$ channels to release Ca^{2+} stored in the ER lumen into the cytoplasm, generating diverse local and global $[Ca^{2+}]_i$ signals (Berridge, 1993, 1997; Hagar and Ehrlich, 2000; Thrower et al., 2001; Taylor and Laude, 2002; Foskett et al., 2007). Whereas much is known regarding the intricate regulation of $InsP_3R$ channel gating by multiple processes—binding of cytoplasmic ligands (Ca^{2+}, $InsP_3$, and ATP^{4-}), posttranslational modifications, interactions with proteins, clustering, differential localization (Joseph, 1996; MacKrill, 1999; Patel et al., 1999; Johenning and Ehrlich, 2002; Foskett et al., 2007; Betzenhauser et al., 2008; Kang et al., 2008; Wagner et al., 2008; Li et al., 2009; Taufiq-Ur-Rahman et al., 2009)—the regulation of $InsP_3R$ channel activity by free Ca^{2+} in the lumen of the ER ($[Ca^{2+}]_{ER}$) remains poorly understood and controversial (Irvine, 1990; Tregear et al., 1991; Ferris et al., 1992; Swillens, 1992; Kindman and Meyer, 1993; Bezprozvanny and Ehrlich, 1994; Bootman, 1994a,b; Swillens et al., 1994; Shuttleworth, 1995; Dupont and Swillens, 1996; Missiaen et al.,

Correspondence to Don-On Daniel Mak: dmak@mail.med.upenn.edu

Abbreviations used in this paper: HEDTA, hydroxyethylethylenediaminetriacetic acid; $InsP_3$, inositol 1,4,5-trisphosphate; $InsP_3R$, $InsP_3$ receptor; lum-out, luminal-side-out; P_o, open probability; r-$InsP_3R$-3, rat type 3 $InsP_3R$.

The Rockefeller University Press $30.00
J. Gen. Physiol. Vol. 140 No. 6 697–716
www.jgp.org/cgi/doi/10.1085/jgp.201210804

1996; Parys et al., 1996; Beecroft and Taylor, 1997; Caroppo et al., 2003; Dawson et al., 2003; Fraiman and Dawson, 2004; Foskett et al., 2007; McCarron et al., 2008; Yamasaki-Mann and Parker, 2011).

The main techniques for studying possible $[Ca^{2+}]_{ER}$ modulation of $InsP_3R$ channel gating have been $^{45}Ca^{2+}$ flux measurements (Nunn and Taylor, 1991, 1992; Tregear et al., 1991; Missiaen et al., 1992a,b; Parys et al., 1993; Beecroft and Taylor, 1997) and fluorescence Ca^{2+} imaging (Combettes et al., 1992, 1996; Missiaen et al., 1992c; Shuttleworth, 1992; Renard-Rooney et al., 1993; Short et al., 1993; Steenbergen and Fay, 1996; Tanimura and Turner, 1996; Tanimura et al., 1998; Caroppo et al., 2003; Higo et al., 2005; McCarron et al., 2008; Yamasaki-Mann and Parker, 2011). Both approaches rely on changes in $[Ca^{2+}]_i$ or $[Ca^{2+}]_{ER}$ to infer channel activity and therefore cannot rigorously control both $[Ca^{2+}]_{ER}$ and $[Ca^{2+}]_i$ simultaneously during experiments. This has made it difficult to differentiate direct effects of $[Ca^{2+}]_{ER}$ on the luminal aspect of the $InsP_3R$ from feed-through effects caused by Ca^{2+} flux through the open channel.

Electrophysiological recordings of single $InsP_3R$ channels allow $InsP_3R$ channel activity to be determined from currents carried by K^+ through open channels (Foskett et al., 2007) and therefore can be performed under rigorously controlled and defined $[Ca^{2+}]_i$ and $[Ca^{2+}]_{ER}$. However, only two electrophysiological studies of the effects of $[Ca^{2+}]_{ER}$ on $InsP_3R$ channel activity have been reported (Bezprozvanny and Ehrlich, 1994; Thrower et al., 2000). Both used $InsP_3R$ reconstituted in lipid bilayers and explored only a limited set of $[Ca^{2+}]_{ER}$, $[Ca^{2+}]_i$, and $[InsP_3]$. Insights about $[Ca^{2+}]_{ER}$ regulation of $InsP_3R$ channels from these studies were limited by insufficient buffering of $[Ca^{2+}]_i$ and the use of nonphysiological concentrations of divalent cations in the luminal solutions in Bezprozvanny and Ehrlich (1994), or inappropriate Ca^{2+} buffering and nonphysiological [KCl] used in Thrower et al. (2000).

Here, we studied systematically the effects of $[Ca^{2+}]_{ER}$ on the activity of single homotetrameric channels of recombinant rat type 3 $InsP_3R$ (r-$InsP_3R$-3) expressed in cells with no endogenous $InsP_3R$ expression (Sugawara et al., 1997; Mak et al., 2005), using nuclear patch-clamp techniques (Mak et al., 2005; Vais et al., 2010a) that record activities of the $InsP_3R$ channel in its native membrane milieu (Foskett et al., 2007) with ionic conditions on both sides of the channel, especially $[Ca^{2+}]_i$ and $[Ca^{2+}]_{ER}$, rigorously controlled. By comparing activities (open probability [P_o]) of type 3 $InsP_3R$ channels in excised luminal-side-out (lum-out) nuclear membrane patches exposed to different $[Ca^{2+}]_{ER}$ by rapid perfusion solution exchange (Vais et al., 2010a), we found that high $[Ca^{2+}]_{ER}$ modulated $InsP_3R$ channel activity. However, our experiments ruled out $[Ca^{2+}]_{ER}$ modulation of $InsP_3R$ channel activity through intrinsic functional Ca^{2+}-binding sites on the luminal side of the channel. Instead, the experimental results were consistent with $[Ca^{2+}]_{ER}$ affecting $InsP_3R$ channel gating solely through the rise in local $[Ca^{2+}]_i$ in the vicinity of the open channel generated by the $[Ca^{2+}]_{ER}$-driven Ca^{2+} flux through the open channel itself, which modulates $InsP_3R$ channel activity through functional cytoplasmic Ca^{2+}-binding sites of the channel.

MATERIALS AND METHODS

Nucleus isolation and nuclear patch-clamp electrophysiology

Generation and maintenance of DT40-KO-r-$InsP_3R$-3 cells (mutant cells derived from chicken B cells with the endogenous genes for all three $InsP_3R$ isoforms knocked out and then stably transfected to express recombinant r-$InsP_3R$-3) were described in Mak et al. (2005). Nuclear patch-clamp experiments were performed using nuclei isolated from DT40-KO-r-$InsP_3R$-3 cells as described previously (Mak et al., 2005). Experiments investigating $InsP_3R$ activity under constant ligand conditions were performed in the on-nucleus configuration (Mak et al., 2007). Excised nuclear membrane patches in the lum-out configuration were obtained from isolated nuclei (Mak et al., 2007) using protocols analogous to those used to obtain inside-out excised patches in plasma membrane patch-clamp experiments. The solution around the excised nuclear membrane patch was rapidly switched multiple times using a solution-switching setup described in Mak et al. (2007).

$InsP_3R$ channel current traces were acquired at room temperature as described previously (Mak et al., 1998), digitized at 5 kHz, and anti-aliasing filtered at 1 kHz. All applied potentials (V_{app}) were measured relative to the bath electrode. All on-nucleus experiments were performed at $V_{app} = -40$ mV. All lum-out experiments were performed at $V_{app} = -30$ mV unless stated otherwise.

Experimental solution composition

All experimental solutions contained 140 mM KCl and 10 mM HEPES, pH to 7.3 with KOH. Because physiological levels of free Mg^{2+} (0–3 mM) have no effects on channel activities (Mak et al., 1999), and to avoid the complicating effects of Mg^{2+} on $InsP_3R$ channel conductance (Mak and Foskett, 1998) and free [ATP] in experimental solutions, Mg^{2+} was not added to any of the solutions used.

All experiments were performed using the same bath solution with free Ca^{2+} concentration ($[Ca^{2+}]_f$) of 70 nM buffered by 0.5 mM BAPTA (1,2-bis(o-aminophenoxy) ethane-*N*,*N*,*N*′,*N*′-tetraacetic acid). All pipette solutions contained 0.5 mM Na_2ATP.

Pipette solutions used in on-nucleus patch-clamp experiments contained various $[Ca^{2+}]_f$ buffered by 0.5 mM Ca^{2+} chelator and $[InsP_3]$ as specified. BAPTA was used for 20 nM < $[Ca^{2+}]_f$ < 600 nM, diBrBAPTA (5,5′-dibromo BAPTA) for 600 nM ≤ $[Ca^{2+}]_f$ ≤ 4 µM, and hydroxyethylethylenediaminetriacetic acid (HEDTA) for $[Ca^{2+}]_f$ > 4 µM. ATP contributed to Ca^{2+} buffering in solutions with $[Ca^{2+}]_f$ > 30 µM (Bers et al., 2010).

Pipette solutions used in lum-out patch-clamp experiments had $[Ca^{2+}]_f$ of either 2 µM buffered by various concentrations of diBrBAPTA or HEDTA as specified, or 55 nM buffered by various concentrations of BAPTA as specified. Four perfusion solutions were used in these experiments: one had $[Ca^{2+}]_f$ of 70 nM buffered by 0.5 mM BAPTA with no ATP; one contained 1.3 mM $CaCl_2$ and 1.5 mM Na_2ATP, so that $[Ca^{2+}]_f$ was buffered to 300 µM according to Max Chelator freeware; and two with no Ca^{2+} chelator, with one containing 1 mM $CaCl_2$ and the other containing 2 mM $CaCl_2$, giving $[Ca^{2+}]_f$ of 550 µM and 1.1 mM, respectively,

according to activity coefficient calculations (Butler, 1968; Vais et al., 2010a).

$[Ca^{2+}]_f$ in all solutions (<100 µM) was confirmed by Ca^{2+}-sensitive dye fluorimetry.

Data analysis

Because there is no Ca^{2+} flux through open $InsP_3R$ channels in steady-state on-nucleus experiments using bath solutions containing only 70 nM $[Ca^{2+}]_f$, there was no possibility of cross talk between channels. Furthermore, we detected no effect of channel clustering on gating of $InsP_3R$ channels expressed in DT40-KO-r-$InsP_3R$-3 cells (Vais et al., 2011). Thus, multi-channel and single-channel current traces were selected for channel P_o and dwell-time analysis using QuB software (Qin et al., 2000a,b). However, because substantial Ca^{2+} flux can be driven through open $InsP_3R$ channels when some perfusion solutions were used in excised lum-out nuclear patch-clamp experiments, only single-channel current traces from such experiments were selected for analysis to avoid complications arising from Ca^{2+} flux through one $InsP_3R$ channel affecting gating behaviors of neighboring active channel(s). We accepted only current records long enough to allow the number of active channels observed to be accurately determined (with >99% confidence) for data analysis (Mak et al., 2001b; Ionescu et al., 2006; Vais et al., 2010b). Only single-channel current traces >15 s were used for channel $P_o > 0.02$. Longer traces were required for lower P_o, so only single-channel traces >1.5 min were used for $P_o \approx 0.005$. Least-square fitting and statistical analysis of data were done with IGOR Pro software (WaveMetrics).

Modeling of the $[Ca^{2+}]_i$ profile in the vicinity of an $InsP_3R$ channel

The $[Ca^{2+}]_i$ profile around an open $InsP_3R$ channel was calculated by considering the open channel as a circular aqueous pore with a diameter of 2.5 nm (Jiang et al., 2002; Serysheva et al., 2003; Wolfram et al., 2010). Magnitudes of the Ca^{2+} current through an open channel (i_{Ca}) in the presence of 140 mM KCl and various $[Ca^{2+}]_i$, $[Ca^{2+}]_{ER}$, and V_{app} were evaluated using the general Goldman–Hodgkin–Katz current equation (Lewis, 1979; Hille, 2001):

$$i_{Ca} = P_{Ca} z_{Ca}^2 \frac{F^2 V_{app}}{RT} \left\{ \frac{[Ca]_i - [Ca]_{ER} \exp\left(-z_{Ca} F V_{app}/RT\right)}{1 - \exp\left(-z_{Ca} F V_{app}/RT\right)} \right\}, \quad (1)$$

where z_{Ca} (= 2) is the valence of Ca^{2+}, F is the Faraday constant, R is the gas constant, T is the absolute temperature, and P_{Ca} is the effective channel permeability for Ca^{2+} through the $InsP_3R$ channel measured experimentally in buffers containing 140 mM KCl (Vais et al., 2010a).

Although the analytical equation obtained by using the approximation in Neher (1986, 1998), Smith (1996), and Naraghi and Neher (1997) can provide a reasonable estimation of the steady-state $[Ca^{2+}]_i$ profile around a Ca^{2+} channel generated by Ca^{2+} flux through the channel buffered by mobile Ca^{2+}-binding chelators (Liu et al., 2010; Vais et al., 2010a), it says nothing about the time scale of the evolution of the $[Ca^{2+}]_i$ profile to reach the steady state. These dynamics then affect the dissipation of the Ca^{2+} profile after the channel closes. Once a channel closes, the profile collapses first to a level that is above basal very quickly but then dissipates toward basal on a slow time scale. Therefore, to follow the time-dependent evolution of the $[Ca^{2+}]_i$ profiles around the channel as it gates, numerical modeling of Ca^{2+} diffusion around the open $InsP_3R$ channel was used to calculate the $[Ca^{2+}]_i$ profiles in the vicinity of the channel under various $[Ca^{2+}]_i$, $[Ca^{2+}]_{ER}$, and V_{app} combinations.

In the simulations, $[Ca^{2+}]_i$ is controlled by spatial diffusion, with the rate equation for $[Ca^{2+}]_i$ at distance r from the channel at time t after the channel opens, $C(r,t)$, given as

$$\frac{\partial C(r,t)}{\partial t} = D_C \nabla^2 C + J + \frac{\partial b}{\partial t}, \quad (2)$$

where J is the Ca^{2+} flux passing through the channel from the ER lumen, D_C is the diffusion coefficient of Ca^{2+} in the medium (= 800 $\mu m^2 s^{-1}$ [Cussler, 1997] for aqueous medium), and b is the free Ca^{2+} buffer concentration.

For mobile Ca^{2+} buffers, $\partial b/\partial t$ is given as

$$\frac{\partial b}{\partial t} = D_b \nabla^2 b + k_{off}(B - b) - k_{on} C b, \quad (3)$$

where B is the total Ca^{2+} buffer concentration, and k_{on} and k_{off} are the rates of Ca^{2+} binding to and dissociating from the buffer, respectively, so that $k_{off}/k_{on} = K_d$ (dissociation constant) of the buffer. D_b is the diffusion coefficient of the mobile buffer.

K_d for diBrBAPTA, HEDTA, and BAPTA is 1.6 µM, 4.7 µM, and 180 nM, respectively. k_{on} for diBrBAPTA, HEDTA, and BAPTA is 450, 4.5, and 450 $\mu M^{-1} s^{-1}$, respectively (Tsien, 1980; Naraghi, 1997). D_b for diBrBAPTA, HEDTA, and BAPTA is 296, 319, and 390 $\mu m^2 s^{-1}$, respectively, estimated from $D_b = D_C \sqrt[3]{M_C/M_b}$, where M_b and M_C are the molecular weights of the buffer and Ca^{2+}, respectively.

i_{Ca} in Eq. 1 is converted into J in Eq. 2 by

$$J = \begin{cases} i_{Ca}/(F z_{Ca} \delta V) & \text{for } r \le r_{ch} \\ 0 & \text{for } r > r_{ch} \end{cases}, \quad (4)$$

where r_{ch} is the radius of the channel pore. For simplicity, the channel is considered to be embedded in an infinite membrane, opening into a semi-infinite cytoplasmic volume. Then, δV is the volume of a hemisphere with radius r_{ch} over the channel. Propagation of Ca^{2+} and mobile buffer (if present) was simulated throughout a homogeneous semi-infinite 3-D cytosolic space.

With spherical symmetry around the channel, the Laplacian of C and b in spherical coordinates is

$$\nabla^2 X(r,t) = \frac{1}{r^2} \frac{\partial}{\partial r} \left(r^2 \frac{\partial X}{\partial r} \right), \quad (5)$$

where $X = C$ or b.

The differential Eqs. 2 and 3 were solved implicitly with a spatial grid size of 0.625 nm using the Tridiagonal Matrix Solver software in a hemispherical volume of a large radius of 10 µm, so that the volume was effectively semi-infinite. The channel opened at $t = 0$ and remained open for the duration of the simulation. Calcium profiles were evolved with 0.1-µs time steps.

To simulate the collapse of the $[Ca^{2+}]_i$ profile after channel closure, the $[Ca^{2+}]_i$ profile was allowed to evolve for 50 ms after the channel opened. Then, J was set equal to 0 for all r at $t = 0$ as the channel closed. The $[Ca^{2+}]_i$ profile was then evolved using the same software with the same time steps for various durations.

RESULTS

Dependence of steady-state $InsP_3R$-3 channel activity on cytoplasmic ligands

To investigate the effects of ER luminal Ca^{2+} concentration ($[Ca^{2+}]_{ER}$) on $InsP_3R$-3 channel gating, we first performed on-nucleus patch-clamp experiments on nuclei isolated from DT40-KO-r-$InsP_3R$-3 cells to characterize the gating behaviors of single recombinant homotetrameric r-$InsP_3R$-3 channels over a wide range of $[InsP_3]$

and $[Ca^{2+}]_i$ in the presence of a physiological level (5 mM) of free ATP, which supports $InsP_3R$ channel gating (Mak et al., 1999, 2001a). In a bath solution with $[Ca^{2+}]_f = 70$ nM and no MgATP to support activity of the SERCA in the outer nuclear membrane, $[Ca^{2+}]_f$ in the perinuclear space of the isolated nuclei (equivalent to the ER lumen topologically) equilibrated with that of the bath solution so that $[Ca^{2+}]_{ER} = 70$ nM in these experiments. The channel with large conductance (~550 pS in 140 mM KCl) observed in the outer nuclear membrane of nuclei isolated from DT40-KO-r-$InsP_3R$-3 cells (Fig. 1) was identified as recombinant $InsP_3R$-3 channel by its requirement of $InsP_3$ for activation (Cheung et al., 2008; Vais et al., 2010a).

In the presence of high (10 µM) $[InsP_3]$, the $InsP_3R$-3 channel exhibited biphasic dependence on $[Ca^{2+}]_i$, with channel P_o increasing as $[Ca^{2+}]_i$ increased until a maximum P_o was reached at $[Ca^{2+}]_i$ of ~2–6 µM. Further increases in $[Ca^{2+}]_i$ inhibited channel P_o (Fig. 1, A and C).

A further increase in $[InsP_3]$ (100 µM) did not change the gating of $InsP_3R$-3 appreciably, indicating that the channel was saturated by 10 µM $InsP_3$ in $[Ca^{2+}]_i$ between 1 and 20 µM (Fig. 1 C). Reduction in $[InsP_3]$ below 10 µM did not affect Ca^{2+} activation of the channel significantly but substantially enhanced the sensitivity of the channel to $[Ca^{2+}]_i$ inhibition so the channel was inhibited at lower $[Ca^{2+}]_i$ (Fig. 1, B and C). This reduced both the maximum channel P_o observed and the range of $[Ca^{2+}]_i$ over which the channel gated appreciably in low $[InsP_3]$ (notably for $[InsP_3] = 1$ µM in Fig. 1 C).

The $[Ca^{2+}]_i$ dependence of $InsP_3R$-3 channel P_o in all $[InsP_3]$ can be well fitted simultaneously for all $[InsP_3]$ investigated by the biphasic Hill equation (Foskett et al., 2007) (Fig. 1 C):

$$P_o = P_{max}\left\{1+\left(\frac{K_{act}}{[Ca^{2+}]_i}\right)^{H_{act}}\right\}^{-1}\left\{1+\left(\frac{[Ca^{2+}]_i}{K_{inh}}\right)^{H_{inh}}\right\}^{-1}, \quad (7)$$

with four of the five parameters retaining the same values: $P_{max} = 1$, $K_{act} = 940$ nM, H_{act} (Hill coefficient for Ca^{2+}

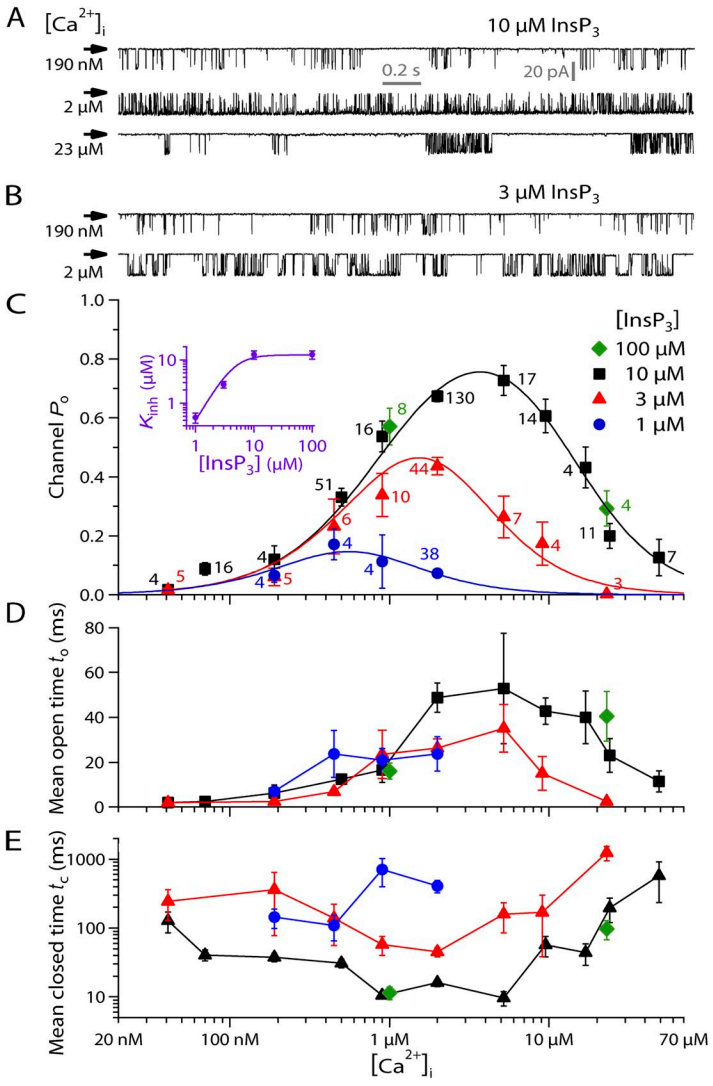

Figure 1. Ligand dependence of gating of single r-$InsP_3R$-3 channels. $V_{app} = -40$ mV. (A) Typical single-channel on-nucleus patch-clamp current traces of $InsP_3R$-3 channels in suboptimal (190 nM), optimal (2 µM), and inhibitory (23 µM) $[Ca^{2+}]_i$ in the presence of saturating (10 µM) $[InsP_3]$, demonstrating biphasic $[Ca^{2+}]_i$ dependence of $InsP_3R$-3 channel activity. Arrow indicates closed-channel baseline current level for these and all subsequent current traces. (B) Typical single-channel on-nucleus patch-clamp current traces in the presence of subsaturating (3 µM) $[InsP_3]$ showing that $[InsP_3]$ reduction has little effect on channel activity at suboptimal (190 nM) $[Ca^{2+}]_i$ but increases channel sensitivity to Ca^{2+} inhibition, so channel activity is substantially decreased at $[Ca^{2+}]_i = 2$ µM. (C) $[Ca^{2+}]_i$ dependence of mean channel P_o in various $[InsP_3]$ as tabulated. Error bars show the SEM in this and all subsequent figures unless stated otherwise. The number of current traces analyzed for each data point is tabulated next to the data point in the same color. Curves are empirical biphasic Hill equation fits to mean P_o data points for various $[InsP_3]$ with the same P_{max}, K_{act}, H_{act}, and H_{inh}. The purple inset shows the dependence of the K_{inh} on $[InsP_3]$. Error bars here show the estimates of fitting errors of K_{inh} derived from the biphasic Hill equation fits. The curve is the empirical simple Hill equation fit of the $[InsP_3]$ dependence. (D and E) $[Ca^{2+}]_i$ dependence of mean open and closed durations of $InsP_3R$ channel in various $[InsP_3]$, derived from the same experimental data used in C. Data points in the same $[InsP_3]$ are connected with lines for clearer presentation.

activation) = 1.3, and H_{inh} (Hill coefficient for Ca^{2+} inhibition) = 1.6. Only K_{inh} varies with [$InsP_3$] (inset in Fig. 1 C). P_{max} from the Hill equation fit of the P_o data is significantly greater than the maximum P_o (0.78) observed in saturating [$InsP_3$]. This indicates that even in saturating [$InsP_3$], the recombinant $InsP_3R$-3 channel in DT40-KO-r-$InsP_3R$-3 cells is not fully activated by $[Ca^{2+}]_i$ before it begins to be inhibited by $[Ca^{2+}]_i$. Because the $[Ca^{2+}]_i$ dependence of the $InsP_3R$-3 channel does not exhibit a clear plateau with channel P_o staying at P_{max} over a broad range of $[Ca^{2+}]_i$, K_{act} and K_{inh} are not uniquely defined by the observed $[Ca^{2+}]_i$ dependence (Foskett et al., 2007). Nevertheless, because P_{max} must be ≤1, the large observed maximum P_o (≈0.78) indicates that the values of K_{act} and K_{inh} derived from the biphasic Hill equation fit are reasonable indications of the apparent affinities of the activating and inhibitory cytoplasmic Ca^{2+}-binding sites of the channel. Thus, the biphasic Hill equation fitting result that only K_{inh} depends on [$InsP_3$] indicates that $InsP_3$ modulates $InsP_3R$-3 gating solely by changing the sensitivity of the channel to Ca^{2+} inhibition (Mak et al., 1998; Foskett et al., 2007). Both Hill coefficients for Ca^{2+} activation and inhibition are moderately >1, suggesting that both Ca^{2+} activation and inhibition are cooperative but not strongly so.

The dependence of K_{inh} on [$InsP_3$] is well described by a simple activating Hill equation (inset in Fig. 1 C):

$$K_{inh} = K_{inh}^{\infty}\left\{1+\left(K_{InsP3}/[InsP_3]\right)^{H_{InsP3}}\right\}^{-1},$$

with K_{inh}^{∞} (K_{inh} in saturating [$InsP_3$]) ≈ 13 µM and K_{InsP3} (half-maximal [$InsP_3$]) ≈ 4.5 µM. H_{InsP3} (Hill coefficient for modulation of K_{inh} by [$InsP_3$]) is ∼2.3. This suggests that $InsP_3$ modulation of $InsP_3R$-3 channel activity is strongly cooperative.

These main features of ligand regulation of the activity of homotetrameric recombinant r-$InsP_3R$-3 channel in DT40-KO-r-$InsP_3R$-3 cells are highly reminiscent of those of a variety of $InsP_3R$ channels in different cell systems examined using the same approach: endogenous *Xenopus laevis* type 1 $InsP_3R$ ($InsP_3R$-1) channel in oocytes, recombinant r-$InsP_3R$-3 channel expressed in *Xenopus* oocytes, and endogenous insect $InsP_3R$ channel in Sf9 cells (Foskett et al., 2007). However, the r-$InsP_3R$-3 channel in DT40-KO-r-$InsP_3R$-3 cells is significantly less sensitive to $[Ca^{2+}]_i$ and [$InsP_3$] activation than the other channels, with significantly higher K_{act} and K_{InsP3}. Furthermore, the efficacy of $InsP_3$ to activate the channel by reducing its sensitivity to inhibition by $Ca^{2+}{}_i$ is also lowest for r-$InsP_3R$-3 channel in DT40-KO-r-$InsP_3R$-3 cells among $InsP_3R$ channels studied (Foskett et al., 2007), as indicated by its low K_{inh}^{∞}.

Regulation of r-$InsP_3R$-3 channel gating kinetics by cytoplasmic ligands

The $[Ca^{2+}]_i$ dependence of the mean open duration (t_o) of r-$InsP_3R$-3 channels expressed in DT40-KO-r-$InsP_3R$-3 cells loosely mirrors that of channel P_o, with t_o continuously increasing as $[Ca^{2+}]_i$ was increased from 40 nM to ≈1 µM. Within this $[Ca^{2+}]_i$ range, t_o was similar in the same $[Ca^{2+}]_i$ for all [$InsP_3$]. t_o then remained high for a range of $[Ca^{2+}]_i$ extending beyond the point where channel P_o started to be reduced by higher $[Ca^{2+}]_i$. Beyond a threshold $[Ca^{2+}]_i$, t_o started to be reduced by higher $[Ca^{2+}]_i$. The threshold $[Ca^{2+}]_i$ was ≈20 µM in 10 µM $InsP_3$ and ≈6 µM in 3 µM $InsP_3$. Thus, the threshold $[Ca^{2+}]_i$ decreased as [$InsP_3$] was reduced (Fig. 1 D).

Ligand regulation of the mean channel closed duration (t_c) is more complex. In saturating [$InsP_3$], t_c decreased continuously as $[Ca^{2+}]_i$ was increased up to 1 µM, when it reached a minimum of ∼10 ms at $[Ca^{2+}]_i$ ≈ 900 nM, before P_o attained its maximum value. t_c remained at the minimum value as $[Ca^{2+}]_i$ was increased to 6 µM. Then, t_c increased when P_o started to be reduced by rising $[Ca^{2+}]_i$. Unlike t_o, t_c was increased in all $[Ca^{2+}]_i$ as [$InsP_3$] was reduced below saturating levels, except at very low $[Ca^{2+}]_i$ (∼40 nM). As $[Ca^{2+}]_i$ was increased, t_c followed a trend that is the inverse of that of P_o, decreasing until t_c reached its minimum at the $[Ca^{2+}]_i$ at which P_o was maximal, and then increasing as P_o decreased (Fig. 1 E).

These ligand dependencies of the gating characteristics (t_o and t_c) of r-$InsP_3R$-3 in DT40-KO-r-$InsP_3R$-3 cells are markedly more complex than those of other $InsP_3R$ channels examined (Mak et al., 1998, 2001b; Ionescu et al., 2006). For the other channels, t_o remained effectively constant over most of the ranges of [$InsP_3$] and $[Ca^{2+}]_i$ examined, so that once a channel opens, the duration for which it remains open is largely independent of the local $[Ca^{2+}]_i$ and [$InsP_3$]. Ligand modulations of P_o of those channels therefore result mostly from ligand modulations of t_c.

Effects of physiological levels of $[Ca^{2+}]_{ER}$ on $InsP_3R$-3 channel gating

To study possible modulation of $InsP_3R$-3 channel gating by $[Ca^{2+}]_{ER}$, nuclear patch-clamp experiments in the excised lum-out configuration were performed on nuclei from DT40-KO-r-$InsP_3R$-3 cells. The luminal side of $InsP_3R$ channels in the isolated nuclear membrane patches was exposed rapidly and repeatedly to solutions containing different $[Ca^{2+}]_f$ using rapid perfusion solution exchange (Vais et al., 2010a,b). To avoid the complication of Ca^{2+} moving through one active $InsP_3R$ channel affecting the activity of neighboring active channels by raising local $[Ca^{2+}]_i$, only single-channel current traces obtained in these lum-out nuclear patch-clamp experiments were used for analysis.

To detect possible activating or inhibitory effects of $[Ca^{2+}]_{ER}$ on $InsP_3R$ channel gating, we first used a pipette solution containing subsaturating (3 µM) [$InsP_3$] and optimal (2 µM) $[Ca^{2+}]_i$ buffered by 0.5 mM diBrBAPTA. Active $InsP_3R$-3 channels were exposed alternately to

$[Ca^{2+}]_{ER}$ of 70 nM, a sub-physiological $[Ca^{2+}]_{ER}$ in which no Ca^{2+} flux flowed from the luminal side of the channels to the cytoplasmic side, and 300 µM, a physiological $[Ca^{2+}]_{ER}$ that drives substantial Ca^{2+} flux through the channels (Vais et al., 2010a). Increasing $[Ca^{2+}]_{ER}$ from 70 nM to 300 µM caused a reduction in the magnitude of the current passing through the active $InsP_3R$-3 channels (Fig. 2 A) because Ca^{2+} acts as permeant channel blocker, reducing K^+ conductance of the channel (Vais et al., 2010a). Returning $[Ca^{2+}]_{ER}$ to 70 nM restored the channel current magnitude (Fig. 2 B). Such changes in channel current size were used in all experiments to mark the time when the perfusion solution exchange was completed at the luminal side of the active $InsP_3R$ channels.

Besides the reduction in channel conductance, the jump in $[Ca^{2+}]_{ER}$ from 70 nM to 300 µM caused a significant decrease in channel P_o (Fig. 2 A), which was reversed when $[Ca^{2+}]_{ER}$ was returned to 70 nM (Fig. 2 B). This effect of $[Ca^{2+}]_{ER}$ on channel P_o was quantified by the ratio of the P_o observed when $[Ca^{2+}]_{ER}$ = 300 µM (P_o(300 µM)) to that when $[Ca^{2+}]_{ER}$ = 70 nM (P_o(70 nM)), evaluated immediately before and after each perfusion solution switch (Fig. 2, A and B). With $[InsP_3]$ = 3 µM and $[Ca^{2+}]_i$ = 2 µM, the $InsP_3R$ channel was significantly less active in $[Ca^{2+}]_{ER}$ = 300 µM than in $[Ca^{2+}]_{ER}$ = 70 nM, so the mean P_o ratio ($\langle P_o(300\ \mu M)/P_o(70\ nM)\rangle$; the angle brackets are used to emphasize that this is the mean of the P_o ratios, not the ratio of the mean P_o's at different $[Ca^{2+}]_{ER}$) was significantly lower than unity (Fig. 2 D, red bar). The change in $[Ca^{2+}]_{ER}$ also caused significant changes in both t_o and t_c, so the mean t_o and t_c ratios ($\langle t_o(300\ \mu M)/t_o(70\ nM)\rangle$ and $\langle t_c(300\ \mu M)/t_c(70\ nM)\rangle$, respectively) are both significantly different from unity (Fig. 2, E and F, red bars).

The observed inhibition of $InsP_3R$ gating by elevated $[Ca^{2+}]_{ER}$ can be caused by luminal free Ca^{2+} (Ca^{2+}_{ER}) binding to an inhibitory site on the luminal side of the channel. Alternatively, it could be caused by Ca^{2+} binding to cytoplasmic sites on the $InsP_3R$ channel because of local $[Ca^{2+}]_i$ in the vicinity of the pore elevated by Ca^{2+} flux driven through the channel by the high $[Ca^{2+}]_{ER}$. Because $[Ca^{2+}]_i$ in the pipette solution used (2 µM) optimally activates $InsP_3R$ channels in 3 µM $InsP_3$, a rise in local $[Ca^{2+}]_i$ near the channel is predicted to reduce P_o caused by Ca^{2+} binding to the inhibitory Ca^{2+}-binding sites on the cytoplasmic side of the channel (Foskett et al., 2007).

$[Ca^{2+}]_{ER}$ inhibition of $InsP_3R$ channel activity is abolished by saturating $[InsP_3]$ but restored by higher $[Ca^{2+}]_{ER}$

To better characterize the observed $[Ca^{2+}]_{ER}$ regulation of $InsP_3R$ channel activity, we investigated the $[InsP_3]$ dependence of the effect of $[Ca^{2+}]_{ER}$ by using pipette solutions containing different $[InsP_3]$ in our lum-out nuclear patch-clamp experiments. Inhibition of $InsP_3R$

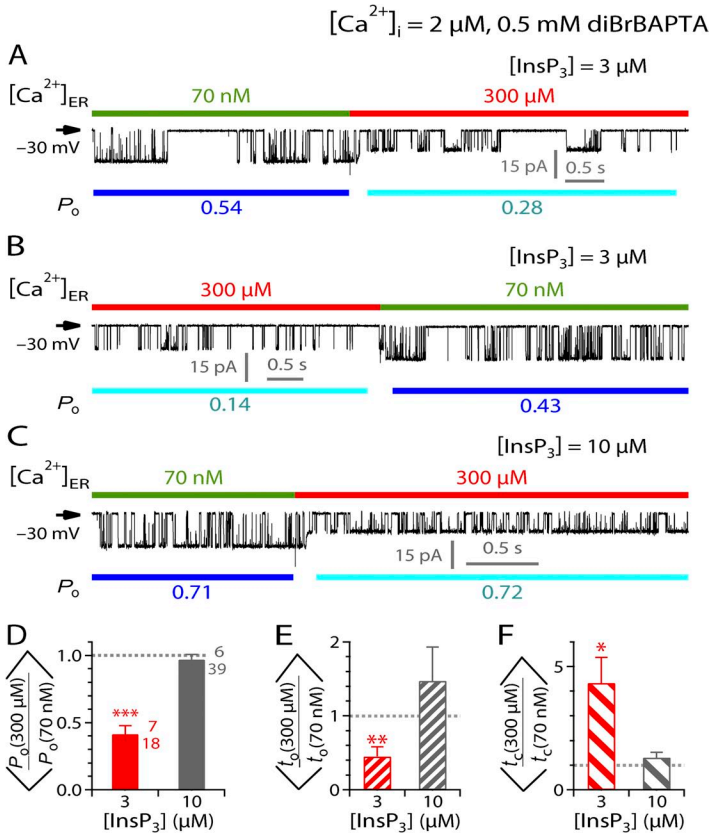

Figure 2. Effects of $[Ca^{2+}]_{ER}$ on $InsP_3R$-3 channel activity in various $[InsP_3]$. (A–C) Typical single-channel current traces from excised lum-out nuclear membrane patches recorded during a rapid switch of $[Ca^{2+}]_{ER}$ by perfusion solution exchange. For clarity, compositions of pipette solutions ($[Ca^{2+}]_i$, concentration and nature of Ca^{2+} chelator used, $[InsP_3]$) common to all experiments presented in this figure (current traces and bar graphs) are tabulated at the top of the figure. Pipette solution composition(s) specific to each current trace is tabulated at the top of the corresponding current trace. In each current trace, V_{app} used is tabulated at left, color bars at the top indicate $[Ca^{2+}]_{ER}$ in the perfusion solutions, and blue bars at the bottom indicate segments used for evaluating the channel P_o tabulated below. In these figures, short current segments were plotted to show the $InsP_3R$ channel gating more clearly. The mean P_o, t_o, and t_c ratios (discussed in Results and Discussion, and shown in bar graphs) were derived from current segments that are significantly longer to ensure that only single-channel nuclear patch current traces were used (see Materials and methods). (D–F) Bar graphs of mean ratios of channel P_o, t_o, and t_c, respectively, observed before and after $[Ca^{2+}]_{ER}$ switching between 70 nM and 300 µM for different $[InsP_3]$. Numbers beside the bars are the number of experiments (top) and perfusion solution switches (bottom) analyzed. ***, **, and * mark significant deviation of a ratio from unity (P < 0.005, 0.01, and 0.05, respectively; paired *t* test). These symbols and conventions are also used for Figs. 3–6, and 8 and 9. For clarity, bars of the same color in these figures correspond to the same set of data obtained under the same experimental conditions.

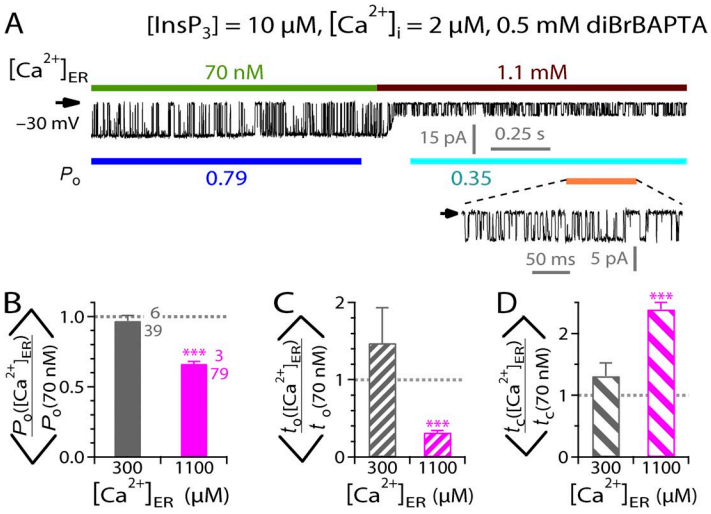

Figure 3. Modulation of $InsP_3R$ channel activity by various $[Ca^{2+}]_{ER}$ in saturating $[InsP_3]$. (A) A typical single-channel current trace recorded during a switch of $[Ca^{2+}]_{ER}$ from 70 nM to 1.1 mM. Note the substantially smaller channel current when $[Ca^{2+}]_{ER}$ = 1.1 mM as a result of the blocking of the channel by permeant Ca^{2+}. A part of the current trace (indicated by an orange line) is shown with larger current and time scales in the inset to show the details of channel gating in $[Ca^{2+}]_{ER}$ = 1.1 mM. (B–D) Bar graphs of mean ratios of channel P_o, t_o, and t_c observed before and after $[Ca^{2+}]_{ER}$ switches between 70 nM and 300 μM or 1.1 mM, as indicated.

channel gating by raising $[Ca^{2+}]_{ER}$ from 70 nM to 300 μM was abrogated in the presence of saturating $[InsP_3]$ (10 μM) (Fig. 2 C), so the mean P_o, t_o, and t_c ratios observed were not significantly different from unity (Fig. 2, D–F, gray bars). In contrast, even in saturating $[InsP_3]$, $InsP_3R$ channel activity was still substantially inhibited when $[Ca^{2+}]_{ER}$ was raised to higher (1.1 mM) levels (Fig. 3 A), with mean P_o ratio significantly less than unity (Fig. 3 B) because of both longer t_c and shorter t_o (Fig. 3, C and D). This is similar to the suppression of channel gating by $[Ca^{2+}]_{ER}$ jumping from 70 nM to 300 μM in subsaturating (3 μM) $[InsP_3]$ (Fig. 2). Accordingly, if the inhibitory effect of high $[Ca^{2+}]_{ER}$ on channel P_o is mediated by some luminal Ca^{2+}-binding site(s) on the channel, the site must be allosterically coupled to the $InsP_3$-binding sites on the cytoplasmic side of the channel so that channel activation by $InsP_3$ binding to its cytoplasmic site and channel inhibition by Ca^{2+} binding to the luminal site are mutually antagonistic. Alternatively, if the $[Ca^{2+}]_{ER}$ effect is mediated by the Ca^{2+} flux through the channel, the lack of effect on channel gating of $[Ca^{2+}]_{ER}$ jump from 70 nM to 300 μM in the presence of saturating $[InsP_3]$ can be accounted for by the $InsP_3$-induced reduction in sensitivity of $InsP_3R$ to $[Ca^{2+}]_i$ inhibition. In this scenario, a rise in local $[Ca^{2+}]_i$ caused by Ca^{2+} flux driven through the channel by $[Ca^{2+}]_{ER}$ of 300 μM that inhibits $InsP_3R$ channel gating in subsaturating $[InsP_3]$ is not sufficient to affect channel gating, as saturating $[InsP_3]$ reduces the sensitivity of the channel to $[Ca^{2+}]_i$ inhibition. However, the higher rise in local $[Ca^{2+}]_i$ driven by a higher $[Ca^{2+}]_{ER}$ of 1.1 mM can still cause suppression of channel activity, even in the presence of saturating $[InsP_3]$.

$[Ca^{2+}]_i$ dependence of the modulation of $InsP_3R$ channel P_o by $[Ca^{2+}]_{ER}$

To identify the mechanisms underlying the regulation of $InsP_3R$ channel activity by $[Ca^{2+}]_{ER}$, we investigated the $[Ca^{2+}]_i$ dependence of the effect. If the observed $[Ca^{2+}]_{ER}$ modulation of $InsP_3R$ channel activity is mediated by cytoplasmic Ca^{2+}-binding sites of the channel, $[Ca^{2+}]_{ER}$ modulation should be consistent with the biphasic $[Ca^{2+}]_i$ regulation of $InsP_3R$ channel P_o (Fig. 1 C). Accordingly, when a pipette solution containing suboptimal low $[Ca^{2+}]_i$ is used instead of one with optimal $[Ca^{2+}]_i$, the rise in local $[Ca^{2+}]_i$ caused by the Ca^{2+} flux

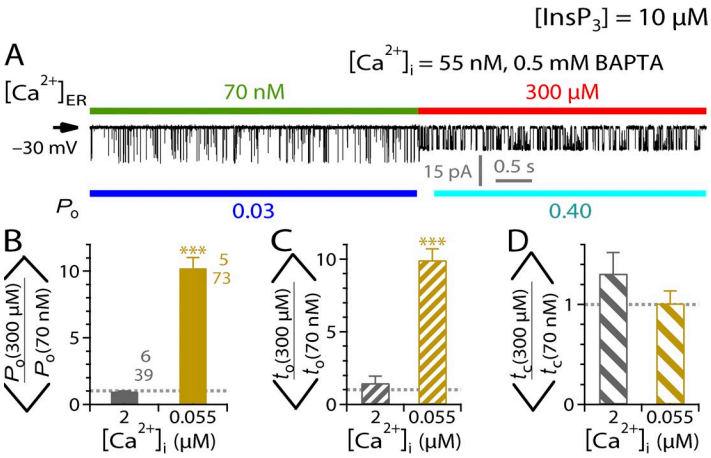

Figure 4. Effects of $[Ca^{2+}]_i$ on $[Ca^{2+}]_{ER}$ modulation of $InsP_3R$ channel activity. (A) A typical single-channel lumout patch-clamp current trace recorded during a switch of $[Ca^{2+}]_{ER}$ from 70 nM to 300 μM by perfusion solution exchange in suboptimal (55 nM) $[Ca^{2+}]_i$. (B–D) Bar graphs of mean ratios of channel P_o, t_o, and t_c, respectively, observed before and after $[Ca^{2+}]_{ER}$ switches between 70 nM and 300 μM for different $[Ca^{2+}]_i$. $[Ca^{2+}]_i$ was buffered to 2 μM by 0.5 mM diBrBAPTA and to 55 nM by 0.5 mM BAPTA.

driven through the open channel by high $[Ca^{2+}]_{ER}$ is expected to activate instead of inhibit channel gating. Indeed, when excised lum-out experiments were performed with saturating (10 µM) $[InsP_3]$ and suboptimal low (55 nM) $[Ca^{2+}]_i$ in the pipette solution, the activity of the $InsP_3R$ channel was significantly enhanced when $[Ca^{2+}]_{ER}$ was switched from 70 nM to 300 µM (Fig. 4 A), as reflected in a mean P_o ratio significantly larger than unity (Fig. 4 B) mainly caused by increase in t_o (Fig. 4 C) while t_c remained unaltered (Fig. 4 D). This observation is difficult to account for with the hypothesis of a luminal Ca^{2+}-binding site on the $InsP_3R$ channel regulating its activity.

$[Ca^{2+}]_{ER}$ modulation of $InsP_3R$ channel P_o depends on the magnitude of the Ca^{2+} flux

To further confirm that rise in local $[Ca^{2+}]_i$ in the vicinity of the channel pore caused by feed-through Ca^{2+} flux driven by high $[Ca^{2+}]_{ER}$ modulates $InsP_3R$ channel significantly by Ca^{2+} binding to cytoplasmic sites on the channel, we investigated whether channel activity would be affected if the magnitude of the Ca^{2+} flux through the $InsP_3R$ channel was altered by changing V_{app} only, with $[Ca^{2+}]_{ER}$ kept the same. In all previous experiments, $V_{app} = -30$ mV. This V_{app} drove Ca^{2+} from the bath solution through the channel to the pipette solution, in the same direction as the $[Ca^{2+}]_f$ gradient when the perfusion solution contained $[Ca^{2+}]_{ER}$ of 300 µM. When the polarity of V_{app} is reversed ($V_{app} = +30$ mV), the applied V_{app} opposes the $[Ca^{2+}]_f$ gradient. Although this change in V_{app} polarity is insufficient to reverse the direction of the Ca^{2+} flux through the channel, it reduces the magnitude of the flux and therefore diminishes the rise in local $[Ca^{2+}]_i$ around the channel pore. In excised lum-out nuclear patch-clamp experiments with saturating $[InsP_3]$ (10 µM) and suboptimal $[Ca^{2+}]_i$ (70 nM), jumps of $[Ca^{2+}]_{ER}$ from 70 nM to 300 µM with $V_{app} = +30$ mV still enhanced $InsP_3R$ channel activity (Fig. 5 A) in a qualitatively similar way as in $V_{app} = -30$ mV, giving a mean P_o ratio significantly larger than unity (Fig. 5 B) solely by prolonging t_o (Fig. 5, C and D). However, the increases in channel P_o and t_o were substantially less in $V_{app} = +30$ mV than those observed with $V_{app} = -30$ mV (Fig. 5, B and C).

$[Ca^{2+}]_{ER}$ modulation of $InsP_3R$ channel P_o depends on cytoplasmic Ca^{2+}-buffering conditions

Our experiments so far have demonstrated convincingly that most of the effects of $[Ca^{2+}]_{ER}$ on $InsP_3R$ channel activity are mediated by the Ca^{2+} flux driven by $[Ca^{2+}]_{ER}$ to raise local $[Ca^{2+}]_i$ to modify $InsP_3R$ channel activity through the cytoplasmic-activating and inhibitory Ca^{2+}-binding sites on the channel. We next performed experiments to examine more closely the existence of an intrinsic functional regulatory Ca^{2+}-binding site on the luminal side of the channel. We investigated the effects of cytoplasmic Ca^{2+}-buffering conditions on $[Ca^{2+}]_{ER}$ modulation of channel activity in optimal $[Ca^{2+}]_i$ (2 µM) and subsaturating $[InsP_3]$ (3 µM). In all previous experiments involving $[Ca^{2+}]_i = 2$ µM, $[Ca^{2+}]_i$ in the pipette (cytoplasmic) solution was buffered by 0.5 mM of the fast Ca^{2+} chelator diBrBAPTA (Ca^{2+} binding rate k_{on} of ~450 $\mu M^{-1}s^{-1}$; Naraghi, 1997). In weaker buffering conditions in which $[Ca^{2+}]_i$ was buffered to 2 µM by a low concentration (0.1 mM) of the slower Ca^{2+} chelator HEDTA (k_{on} of ~4.5 $\mu M^{-1}s^{-1}$) (Naraghi, 1997), suppression of channel activity when $[Ca^{2+}]_{ER}$ was raised from 70 nM to 300 µM was more profound than that observed in 0.5 mM diBrBAPTA (Fig. 6 A). Accordingly, the mean P_o ratio was significantly lower under weak cytoplasmic Ca^{2+}-buffering conditions than under the normally used buffering conditions, even though $[Ca^{2+}]_i$ was kept at 2 µM (Fig. 6 C). This is solely because of a significant increase in t_c (Fig. 6, D and E). In contrast, the inhibitory effects of the same $[Ca^{2+}]_{ER}$ jump were completely abolished when cytoplasmic Ca^{2+} was strongly buffered at 2 µM with a high concentration (5 mM) of diBrBAPTA (Fig. 6 B), giving mean P_o, t_o, and t_c ratios not significantly different from unity (Fig. 6, C–E). Control experiments

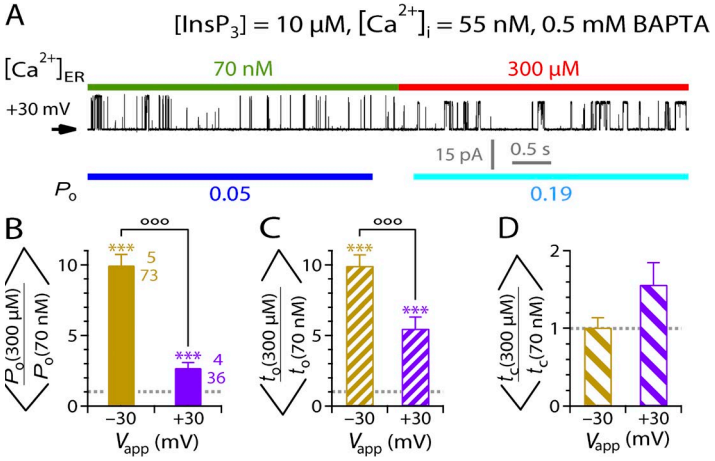

Figure 5. $[Ca^{2+}]_{ER}$ modulation of $InsP_3R$-3 channel activity depends on magnitude of Ca^{2+} flux through the open-channel pore. (A) A typical single-channel lum-out nuclear patch-clamp current trace recorded during a switch of $[Ca^{2+}]_{ER}$ from 70 nM to 300 µM in $V_{app} = +30$ mV. Note that the change in channel current size as the result of the change in $[Ca^{2+}]_{ER}$ was smaller. This is because of the reduction in Ca^{2+} flux through the channel by the positive V_{app}. (B–D) Bar graphs of mean ratios of channel P_o, t_o, and t_c observed before and after $[Ca^{2+}]_{ER}$ switches between 70 nM and 300 µM in $V_{app} = \pm 30$ mV. ooo indicates statistically significant difference between the two ratios connected by the bracket ($P < 0.005$; unpaired t test).

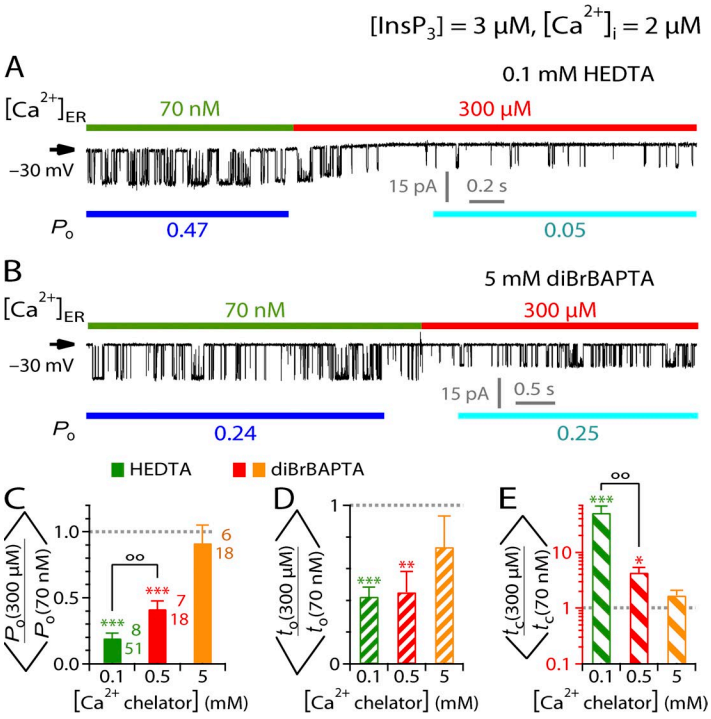

Figure 6. Effects of cytoplasmic Ca^{2+}-buffering conditions on $[Ca^{2+}]_{ER}$ modulation of $InsP_3R$ channel activity. (A and B) Typical single-channel lum-out nuclear patch-clamp current traces recorded during switches of $[Ca^{2+}]_{ER}$ from 70 nM to 300 μM in different cytoplasmic Ca^{2+}-buffering conditions. (C–E) Bar graphs of mean ratios of P_o, t_o, and t_c, respectively, observed before and after $[Ca^{2+}]_{ER}$ switches between 70 nM and 300 μM for different cytoplasmic Ca^{2+}-buffering conditions. ^{oo} indicates statistically significant difference between the two ratios connected by the bracket ($P < 0.01$; unpaired t test). Note the logarithmic scale used for the t_c axis (in red) in E.

demonstrated that different Ca^{2+}-buffering conditions themselves had no significant effect on P_o in the absence of Ca^{2+} flux through the active channels ($[Ca^{2+}]_{ER}$ = 70 nM) in both on-nucleus and excised lum-out configurations (Fig. 7).

If $[Ca^{2+}]_{ER}$ modulation of channel P_o is mediated by luminal Ca^{2+}-binding site(s), it is difficult to conceive how such a luminal site(s) could be sensitive to Ca^{2+} buffering on the cytoplasmic side by artificial chemical Ca^{2+} chelators that are not naturally found in vivo. Furthermore, the complete abolition of the effect of physiological $[Ca^{2+}]_{ER}$ (300 μM) on channel activity by sufficiently strong cytoplasmic Ca^{2+} buffering suggests that there is no luminal Ca^{2+}-binding site intrinsic to the $InsP_3R$, activating or inhibitory, that is sensitive to 300 μM $[Ca^{2+}]_{ER}$.

Complete abrogation of modulatory effects of $[Ca^{2+}]_{ER}$ in the physiological range on $InsP_3R$ channel activity

To determine if $[Ca^{2+}]_{ER}$ in the upper limits of the physiological range could possibly inhibit $InsP_3R$ channel activity through a luminal Ca^{2+}-binding site on the channel, we looked for inhibitory effects on $InsP_3R$ channel activity by $[Ca^{2+}]_{ER}$ jumps from 70 nM to 1.1 mM (higher than most observed $[Ca^{2+}]_{ER}$; Button and Eidsath, 1996; Bygrave and Benedetti, 1996; Meldolesi and Pozzan, 1998; Yu and Hinkle, 2000) that were independent of the rise in $[Ca^{2+}]_i$ resulting from Ca^{2+} flux passing through the open $InsP_3R$ channel. In excised lum-out nuclear patch-clamp experiments with V_{app} = +30 mV (to reduce the magnitude of the Ca^{2+} flux through the open channel) and pipette solution containing saturating (10 μM) $[InsP_3]$ and optimal (2 μM) $[Ca^{2+}]_i$ buffered by

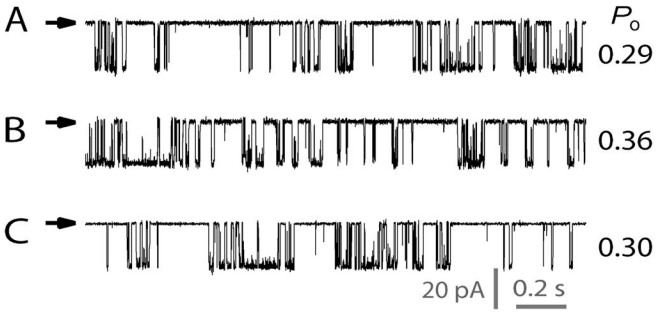

Figure 7. $InsP_3R$ channel P_o is independent of cytoplasmic Ca^{2+}-buffering conditions in the absence of Ca^{2+} flux through the channel. (A–C) Typical single-channel on-nucleus patch-clamp current traces with $[Ca^{2+}]_i$ in pipette solutions buffered to 2 μM by 5 mM diBrBAPTA (A), 0.5 mM diBrBAPTA (B), or 0.1 mM HEDTA (C). $[InsP_3]$ = 3 μM and V_{app} = −40 mV. Bath solution contained $[Ca^{2+}]_{ER}$ = 70 nM. (D) Mean $InsP_3R$ channel P_o for $[InsP_3]$ = 3 μM and $[Ca^{2+}]_i$ = 2 μM in various cytoplasmic Ca^{2+}-buffering conditions for on-nucleus (closed bars) and excised lum-out (open bars) patch-clamp experiments. Excised lum-out patches were perfused with solution containing $[Ca^{2+}]_{ER}$ = 70 nM. H stands for HEDTA, and dB stands for diBrBAPTA. No statistically significant difference exists between P_o in any two of the three Ca^{2+}-buffering conditions plotted for on-nucleus or lum-out experiments (ANOVA).

5 mM diBrBAPTA (to reduce the rise in $[Ca^{2+}]_i$ caused by the Ca^{2+} flux), $[Ca^{2+}]_{ER}$ jumps from 70 nM to 1.1 mM did not affect $InsP_3R$ channel gating (Fig. 8 A), so that the mean P_o, t_o, and t_c ratios observed were not significantly different from unity (Fig. 8, B–D).

We also checked whether the activating effects of $[Ca^{2+}]_{ER}$ on $InsP_3R$ channel activity observed in suboptimal (55 nM) $[Ca^{2+}]_i$ (Fig. 4) could be completely abrogated by a combination of positive V_{app} and strong cytoplasmic Ca^{2+} buffering. Unlike the inhibitory effects, $[Ca^{2+}]_{ER}$ jumps from 70 nM to 550 µM (maximal $[Ca^{2+}]_{ER}$ observed in many cell types; Button and Eidsath, 1996; Bygrave and Benedetti, 1996; Meldolesi and Pozzan, 1998; Yu and Hinkle, 2000) still enhanced $InsP_3R$ channel activity in excised lum-out nuclear patch-clamp experiments with V_{app} = +30 mV and pipette solution containing saturating (10 µM) $[InsP_3]$ and suboptimal (55 nM) $[Ca^{2+}]_i$ buffered by 10 mM BAPTA (Fig. 9 A), so that the mean P_o observed was significantly higher than unity (Fig. 9 D), mostly because of longer t_o (Fig. 9, E and F). However, increasing V_{app} further to +50 mV substantially diminished the activating effects of the $[Ca^{2+}]_{ER}$ jumps (Fig. 9 B), with a mean P_o ratio that is much lower although still significantly larger than unity (Fig. 9 D), which is caused by the t_o ratio that is significantly greater than unity (Fig. 9, E and F). At V_{app} = +70 mV, the activating effects of the $[Ca^{2+}]_{ER}$ jumps were completely abrogated so that the mean P_o, t_o, and t_c ratios were not different from unity (Fig. 9, D–F).

In the experiments investigating the abrogation of activating effects of $[Ca^{2+}]_{ER}$ changes, $[Ca^{2+}]_{ER}$ was increased to 550 µM rather than 1.1 mM because using high concentrations of Ca^{2+} chelator in the pipette solution did not reduce the activating effects of $[Ca^{2+}]_{ER}$ effectively. This is probably because the cytoplasmic activating Ca^{2+}-binding site is located close to the channel pore (see Discussion). To abrogate the effects of $[Ca^{2+}]_{ER}$ jumps to 1.1 mM as in other experiments would require using V_{app} of >70 mV, which severely compromised the integrity of the gigaohm seal between the isolated nuclear membrane patch and the patch-clamp microelectrode.

Collectively, the total abrogation of both the inhibitory effects (in optimal $[Ca^{2+}]_i$ = 2 µM) and the activating effects (in suboptimal $[Ca^{2+}]_i$ = 55 nM) of physiological levels of $[Ca^{2+}]_{ER}$ in conditions that only affected the magnitude of the Ca^{2+} flux through the channel and the changes in $[Ca^{2+}]_i$ demonstrates that there is no regulatory Ca^{2+}-binding site sensitive to physiological $[Ca^{2+}]_{ER}$ on the luminal side of the $InsP_3R$ channel.

DISCUSSION

This study is the first investigation of the effects of $[Ca^{2+}]_{ER}$ on single-channel activity of $InsP_3R$ using the nuclear patch-clamp approach. Previously, two electrophysiological studies explored the effects of $[Ca^{2+}]_{ER}$ using reconstituted cerebellar type 1 $InsP_3R$ channels in planar lipid bilayers. In the first study (Bezprozvanny and Ehrlich, 1994), the cytoplasmic solution contained no permeant ion, with 55 mM Ba^{2+}, Mg^{2+}, Sr^{2+}, or a combination of Ca^{2+} and Sr^{2+} in the luminal solutions used as the main charge carrier. Channel P_o was significantly reduced as $[Ca^{2+}]_{ER}$ was increased from 300 µM to 44 mM. It was suggested that feed-through effects of $[Ca^{2+}]_{ER}$-driven Ca^{2+} flux through the channel contributed to the inhibition of $InsP_3R$ channel activity, but the existence of a luminal inhibitory Ca^{2+} site could not be conclusively ruled out because of insufficient $[Ca^{2+}]_i$ buffering by only 1 mM EGTA. The relevance of this study was further diminished by the nonphysiological ionic compositions used, which rendered it questionable whether the magnitude of Ca^{2+} flux and therefore the resulting changes in $[Ca^{2+}]_i$ resembled those in physiological ionic conditions. In the second study (Thrower et al., 2000), 500 mM K^+ was present in all solutions with $[Ca^{2+}]_i$ buffered to 0.2–0.3 µM by either 10 mM HEDTA or 1.7 mM BAPTA. The conclusion of the study that Ca^{2+}_{ER} affects $InsP_3R$ channel gating through direct interaction

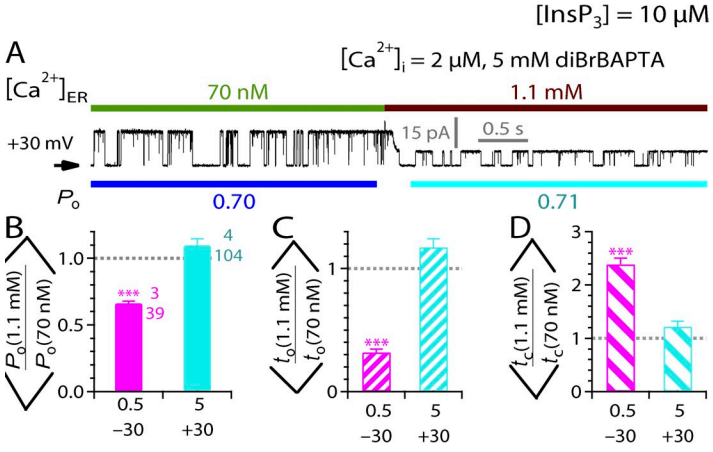

Figure 8. Abrogation of inhibition of $InsP_3R$-3 channel activity by physiological levels of $[Ca^{2+}]_{ER}$. (A) A typical single-channel current trace recorded during a switch of $[Ca^{2+}]_{ER}$ from 70 nM to 1.1 mM. (B–D) Bar graphs of mean ratios of channel P_o, t_o, and t_c observed before and after $[Ca^{2+}]_{ER}$ switches between 70 nM and 1.1 mM, showing the abrogation of inhibitory effects of 1.1 mM $[Ca^{2+}]_{ER}$ on $InsP_3R$ channel activity in the presence of stronger cytoplasmic Ca^{2+} buffering (5 mM BAPTA) and smaller Ca^{2+} flux through the channel as a result of positive V_{app}. Labels on the x axes indicate [diBrBAPTA] in mM (top) and V_{app} in mV (bottom).

with the luminal face of the channel was critically undermined by technical difficulties (brief and inconsistent channel activities, multiple conductance substates), a mostly qualitative description of channel activity (no quantitative P_o or t_o-t_c analysis), and the inappropriate use of Ca^{2+} buffers (HEDTA cannot effectively buffer $[Ca^{2+}]_i$ at 0.2–0.3 µM despite the high concentrations used because of its low Ca^{2+} affinity; BAPTA has the right Ca^{2+} affinity, but only a low concentration was used).

In this study, modulation of $InsP_3R$ channel activity by $[Ca^{2+}]_{ER}$ was examined under rigorously controlled $[Ca^{2+}]_i$, $[Ca^{2+}]_{ER}$, $[InsP_3]$, and cytoplasmic Ca^{2+}-buffering conditions in excised lum-out nuclear patch-clamp experiments with perfusion solution exchange. The observed dependencies of $[Ca^{2+}]_{ER}$ modulation of channel activity on $[InsP_3]$ (Fig. 2), $[Ca^{2+}]_{ER}$ (Fig. 3), $[Ca^{2+}]_i$ (Fig. 4), V_{app} (Fig. 5), and cytoplasmic Ca^{2+}-buffering conditions (Fig. 6), and the total abrogation of the effects of $[Ca^{2+}]_{ER}$ on channel activity by conditions that affect the rise in local $[Ca^{2+}]_i$ caused by the Ca^{2+} flux but not $[Ca^{2+}]_{ER}$ itself (Figs. 6, 8, and 9), together demonstrate that $InsP_3R$ channel activity is regulated solely by the feed-through effects of the $[Ca^{2+}]_{ER}$-driven Ca^{2+} flux through the open channel, raising $[Ca^{2+}]_i$ in the microdomain around the channel to alter P_o of the channel through its cytoplasmic activating and inhibitory Ca^{2+}-binding sites, and not by direct binding of Ca^{2+} to the luminal side of the $InsP_3R$ channel.

The observed modulation of channel activity by $[Ca^{2+}]_{ER}$-driven Ca^{2+} flux through the channel itself provides insights regarding the kinetics of $[Ca^{2+}]_i$ regulation of $InsP_3R$ channel gating. From these insights and others from previous studies of ligand regulation of $InsP_3R$ channel gating, we develop below the concept of the effective time-averaged $[Ca^{2+}]_i$ profile around the channel caused by Ca^{2+} flux through the channel itself when it is gating. With that concept, and using channel P_o observed in the presence of various $[Ca^{2+}]_{ER}$-driven Ca^{2+} fluxes under various $[Ca^{2+}]_i$, $[Ca^{2+}]_{ER}$, and $[InsP_3]$, we then estimate the distances between the channel pore and the cytoplasmic regulatory Ca^{2+} sites.

Kinetics of fluctuations of local $[Ca^{2+}]_i$ in the vicinity of the channel pore caused by Ca^{2+} flux through the pore

In a previous study (Vais et al., 2010a), we determined that physiological levels of $[Ca^{2+}]_{ER}$ can drive substantial Ca^{2+} fluxes through an open $InsP_3R$-3 channel. Numeric simulations allow us to follow the changes in the $[Ca^{2+}]_i$ profile around the Ca^{2+}-permeable $InsP_3R$ channel during its gating. The simulations indicate that under our experimental Ca^{2+}-buffering conditions, the $[Ca^{2+}]_i$ profile around an open $InsP_3R$ channel achieves steady-state levels within 100 µs after the channel opens (Fig. 10 A). Furthermore, after a channel closes, the elevated $[Ca^{2+}]_i$ around the channel collapses rapidly and returns to the basal level within 1 ms (Fig. 10 B). Thus, the $[Ca^{2+}]_i$

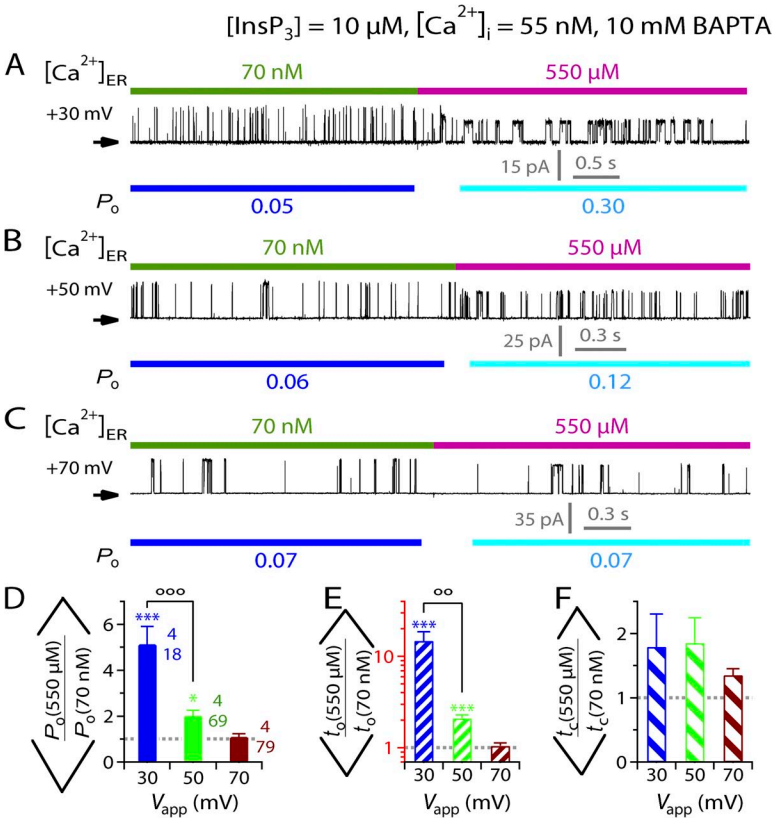

Figure 9. Abrogation of activation of $InsP_3R$-3 channel activity by physiological levels of $[Ca^{2+}]_{ER}$. (A–C) Typical single-current traces recorded during a switch of $[Ca^{2+}]_{ER}$ from 70 nM to 550 µM with different V_{app} used. (D–F) Bar graphs of mean ratios of channel P_o, t_o, and t_c observed before and after $[Ca^{2+}]_{ER}$ switches between 70 nM and 550 µM, showing the abrogation of activating effects of 550 µM $[Ca^{2+}]_{ER}$ on $InsP_3R$ channel activity by increasing positive V_{app} and strong cytoplasmic Ca^{2+} buffering used. ^{ooo} and ^{oo} indicate statistically significant difference between the two ratios connected by the bracket ($P < 0.005$ and 0.01, respectively; unpaired t test). Note the logarithmic scale used for the t_o axis (in red) in E.

profile around an $InsP_3R$ channel fluctuates abruptly between the steady-state open- and closed-channel levels in a quasi-binary manner, with kinetics rigidly dictated by the opening and closing of the channel. This has significant implications for the kinetic properties of $[Ca^{2+}]_i$ regulation of the channel and how $[Ca^{2+}]_{ER}$-driven Ca^{2+} flux through the $InsP_3R$ channel pore can modulate the activity of the channel itself.

Kinetics of cytoplasmic Ca^{2+} activation of $InsP_3R$ channel deduced from the observed enhancement of channel activity by $[Ca^{2+}]_{ER}$-driven Ca^{2+} flux

To derive insights into the kinetics of cytoplasmic Ca^{2+} activation of $InsP_3R$ channel from the observed channel response to $[Ca^{2+}]_{ER}$-driven Ca^{2+} flux through the channel itself, we first consider a hypothetical, extreme kind of response of a Ca^{2+}_i-activated channel to the increase in local $[Ca^{2+}]_i$ at the single activating cytoplasmic Ca^{2+}-binding site of the channel. In this extreme case, the kinetics of channel gating are rigidly dictated by the local $[Ca^{2+}]_i$ at its Ca^{2+} site. To generate this kind of response, the activating latency (interval between local $[Ca^{2+}]_i$ increasing beyond K_{act} and the first resulting opening of the channel, τ_{act}) and the deactivating latency (interval between local $[Ca^{2+}]_i$ decreasing below K_{act} and the last closing of the channel, τ_{deact}) must both be much less than the time scale of channel gating (t_o and t_c), so that the channel opens/closes practically instantaneously after the rise/drop in local $[Ca^{2+}]_i$ at its activating site. Moreover, the channel must remain open as long as its single activating Ca^{2+} site is occupied, and it must remain closed whenever the activating site is vacant, i.e., the gating status (open or closed) of the channel is deterministically dependent on the occupancy of the activating Ca^{2+} site. Given that the $[Ca^{2+}]_i$ profile around a Ca^{2+}-permeable channel is rigidly dictated by the gating of the channel under our experimental conditions (as discussed in the previous section), a lone Ca^{2+}_i-activated, Ca^{2+}-permeable channel in the ER with its gating rigidly dictated by $[Ca^{2+}]_i$ at its activating Ca^{2+} site as described above would not be expected to be activated by Ca^{2+} flux through the channel itself. This is simply because the activating site on the channel must be already occupied when the channel is open and therefore cannot further bind Ca^{2+}. Consequently, the channel cannot be affected by the local $[Ca^{2+}]_i$ elevated by the $[Ca^{2+}]_{ER}$-driven Ca^{2+} flux. Conversely, when its Ca^{2+}-activating site is vacant and available to bind Ca^{2+}, the channel must be closed so that there is no $[Ca^{2+}]_{ER}$-driven Ca^{2+} flux through that channel to activate the channel. Thus, the channel would behave as if there is no Ca^{2+} flux through the open channel.

However, in lum-out nuclear patch-clamp experiments with the pipette solution containing $[Ca^{2+}]_f = 55$ nM and $[InsP_3] = 10$ µM, we observed significant sustained activation of the channel in the presence of high $[Ca^{2+}]_{ER}$ (Figs. 4, A and B, and 5, A and B) that can be completely accounted for by Ca^{2+} flux through the channel raising local $[Ca^{2+}]_i$ at its cytoplasmic activating Ca^{2+} site to enhance its P_o (Fig. 5 A). This observation therefore has nontrivial implications for the kinetics of cytoplasmic Ca^{2+} activation of $InsP_3R$ channel. Most obviously, this indicates that local $[Ca^{2+}]_i$ at the cytoplasmic site does not rigidly dictate the gating of the

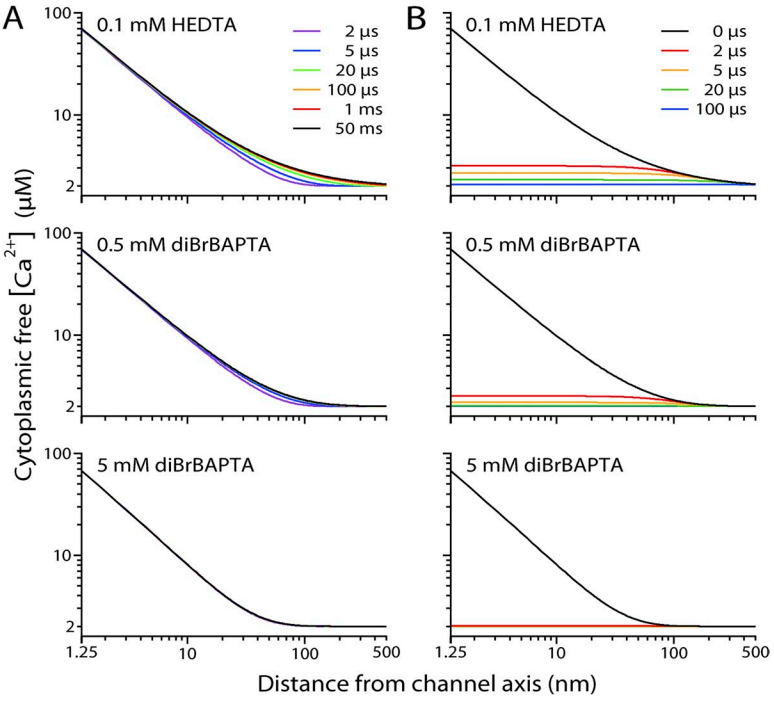

Figure 10. Simulated $[Ca^{2+}]_i$ profiles around an $InsP_3R$ channel (cytoplasmic free $[Ca^{2+}]$ at various distances from the channel pore axis) under various Ca^{2+}-buffering conditions. Buffering conditions are indicated for the profiles shown. $[Ca^{2+}]_{ER}$ = 300 µM. Bulk $[Ca^{2+}]_i$ (far from the channel) = 2 µM. (A) $[Ca^{2+}]_i$ profiles at different t after the channel opens, plotted in different colors as indicated. (B) The channel opened continuously for 50 ms before it closed. Profiles at different t after the channel closed are plotted in different colors as indicated. Even with the weakest buffering (0.1 mM HEDTA), $[Ca^{2+}]_i$ profiles reach steady-state level within 1 ms of the channel opening, and $[Ca^{2+}]_i$ around the channel returns within 100 µs to essentially the level that existed before the channel opened.

channel. Different mechanisms can contribute to uncoupling of the gating kinetics of the channel from changes in $[Ca^{2+}]_i$ at the activating Ca^{2+} site. Most importantly, Ca^{2+} regulates $InsP_3R$ channel activity stochastically, so Ca^{2+} binding to the activating site only induces the channel to adopt a more active kinetic conformation with a higher P_o, but does not always result in channel opening. The channel can open and close with no change in its Ca^{2+}-binding status (Mak et al., 2003). Furthermore, the tetrameric structure of the channel (Foskett et al., 2007) indicates that it has multiple activating Ca^{2+} sites. Thus, the channel can open even when there are vacant activating Ca^{2+} sites on the channel available to detect the elevated local $[Ca^{2+}]_i$ and further enhance channel activity. Another significant factor determining the degree of coupling between local $[Ca^{2+}]_i$ at the activating Ca^{2+} site and the gating of the channel is the kinetics of $Ca^{2+}{}_i$ activation of the channel, i.e., τ_{act} and τ_{deact}. Previous cytoplasmic-side-out nuclear patch-clamp experiments with rapid perfusion exchange studying endogenous $InsP_3R$ channels from insect Sf9 cells (Mak et al., 2007) revealed that in saturating (10 µM) $[InsP_3]$, $InsP_3R$ channels can respond relatively slowly to abrupt changes in $[Ca^{2+}]_i$, with long latencies (τ_{act} of approximately tens of milliseconds and τ_{deact} of approximately a few hundreds of milliseconds). With long response latencies (relative to channel gating t_o and t_c), the channel can open and close, and local $[Ca^{2+}]_i$ around the channel jumps up and down, multiple times during the time the channel takes to respond to one change in $[Ca^{2+}]_i$, thereby effectively uncoupling the $[Ca^{2+}]_i$ at the activating sites from the gating of the channel.

In the other extreme case, in which the gating of the channel is completely uncoupled from the local $[Ca^{2+}]_i$ at the activation sites, instead of responding to the instantaneous $[Ca^{2+}]_i$ resulting from individual channel opening and closing events, the gating of the channel depends only on the time-averaged $[Ca^{2+}]_i$ at the sites. Over a long period T ($>>\tau_{act}$, τ_{deact}, t_o, t_c), a vacant activating Ca^{2+} site on the channel will on average be exposed to the steady-state open-channel $[Ca^{2+}]_i$ (because of the open-channel Ca^{2+} current, i_{Ca}, driven by the electrochemical gradient across the channel) for a period of P_oT, and to the steady-state closed-channel $[Ca^{2+}]_i$ for a period of $(1–P_o)T$. Thus, assuming first-order Ca^{2+} binding to the activating sites, the channel will exhibit steady-state gating kinetics similar to that of a channel with activating sites constantly exposed to a local $[Ca^{2+}]_i$ equivalent to that generated by a Ca^{2+} current of magnitude $P_o i_{Ca}$ passing through the pore.

In reality, the coupling between $InsP_3R$ channel gating and changes of local $[Ca^{2+}]_i$ is partial, lying between the two extremes of total rigid dictation of gating by $[Ca^{2+}]_i$ at the activating sites and complete decoupling with gating unrelated to instantaneous $[Ca^{2+}]_i$ at the sites. Therefore, the activating sites are effectively exposed to a $[Ca^{2+}]_i$ that is equivalent to a time-averaged Ca^{2+} current of magnitude between 0 and $P_o i_{Ca}$.

Besides deducing that $InsP_3R$ channel gating is not rigidly dictated by $[Ca^{2+}]_i$ at the activating sites, other insights about the kinetics of $Ca^{2+}{}_i$ activation of $InsP_3R$ channel can be derived from the observed activating effects of Ca^{2+}-driven Ca^{2+} flux on channel gating. In the present study, in the absence of Ca^{2+} flux with low $[Ca^{2+}]_{ER}$ (70 nM), the $InsP_3R$-3 channel was observed to exhibit low P_o (~0.02–0.05) with short t_o (~2 ms) and long t_c (~50 ms) in constant suboptimal $[Ca^{2+}]_i$ (55 nM), even in saturating $[InsP_3]$ (10 µM) (Figs. 1 C, 4 A, and 9 A). Nevertheless, abrupt and sustained increases in channel P_o and t_o were observed (Figs. 4 A and 9 A) in response to the onset of Ca^{2+} flux through the channel to the cytoplasmic side resulting from $[Ca^{2+}]_{ER}$ being raised to physiological levels. This rapid response indicates that vacant cytoplasmic activating Ca^{2+} sites of the channel were able to capture Ca^{2+} during the first couple of brief channel-opening events after the $[Ca^{2+}]_{ER}$ jump, when the local $[Ca^{2+}]_i$ at the sites was raised by the Ca^{2+} flux and before the channel closed and terminated the Ca^{2+} flux. Thus, the rate of Ca^{2+} binding to the activating sites must be high, suggesting that the Ca^{2+} flux can raise the local $[Ca^{2+}]_i$ at the activating sites to a high level, and therefore the sites are probably located close to the channel pore (see further discussion below).

Another feature of the activating effects of $[Ca^{2+}]_{ER}$ on $InsP_3R$-3 channel gating is that the increase in channel P_o as a result of $[Ca^{2+}]_{ER}$ jumps from 70 nM to physiological levels was mostly achieved by prolonging t_o, with no significant change in t_c (Figs. 4 D, 5 E, and 9 F). It has been suggested that because cytoplasmic regulatory Ca^{2+} sites are inaccessible to $[Ca^{2+}]_{ER}$ when a Ca^{2+}-permeable, $Ca^{2+}{}_i$-regulated channel is closed, the absence of luminal Ca^{2+} site on the channel means that t_c of the channel should not depend on $[Ca^{2+}]_{ER}$ (Laver, 2007a,b). According to this statement, our observation that t_c was not significantly affected by $[Ca^{2+}]_{ER}$ is consistent with a conclusion that the $InsP_3R$ channel has no luminal regulatory Ca^{2+} site. However, the statement is only true for a $Ca^{2+}{}_i$-regulated, Ca^{2+}-permeable channel whose gating is strongly dictated by $[Ca^{2+}]_i$ at its cytoplasmic regulatory Ca^{2+} sites. Because gating of the $InsP_3R$ channel is not rigidly dictated by $[Ca^{2+}]_i$ at its cytoplasmic Ca^{2+}-activating sites, the observation is better interpreted as an indication that under the experimental conditions used in Figs. 4 A, 5 A, and 9 (A and B), the conformations assumed by the channel in the presence and absence of Ca^{2+} flux have similar t_c.

Cytoplasmic inhibitory Ca^{2+} sites also experience an effective time-averaged local $[Ca^{2+}]_i$ due to $[Ca^{2+}]_{ER}$-driven Ca^{2+} flux through the channel

In the extreme case where gating is rigidly dictated by $[Ca^{2+}]_i$ at the regulatory sites, the situation for Ca^{2+}

inhibition is different from that for Ca^{2+} activation for a Ca^{2+}_i-regulated, Ca^{2+}-permeable channel. Whereas activating sites can never experience the flux through the channel (discussed above), the inhibitory sites will be vacant when the channel opens and occupied when the channel is closed. Thus, effectively, the vacant sites will always be exposed to the elevated open-channel local $[Ca^{2+}]_i$ caused by the Ca^{2+} current of magnitude i_{Ca} through the pore.

However, this cannot be true for the $InsP_3R$-3 channel. Even though our experimental observations clearly demonstrated that the channel has no luminal regulatory Ca^{2+}-binding site (Fig. 8), and the rapid collapse of the $[Ca^{2+}]_i$ profile around the channel pore after the channel closes (Fig. 10) means that the cytoplasmic inhibitory Ca^{2+} sites are effectively inaccessible to $[Ca^{2+}]_{ER}$ when the channel is closed, channel t_c still exhibited clear dependence on $[Ca^{2+}]_{ER}$ when the channel was inhibited by rise in $[Ca^{2+}]_i$ caused by Ca^{2+} flux through the open channel (Figs. 2 F, 3 D, and 6 E). Therefore, the gating of the channel cannot be rigidly dictated by $[Ca^{2+}]_i$ at the inhibitory sites. Rather, the observations suggest the presence of uncoupling mechanisms: the tetrameric $InsP_3R$ channel having multiple inhibitory sites that regulate channel P_o stochastically, with Ca^{2+} inhibition latency and the latency of channel recovery from Ca^{2+} inhibition both significantly longer than the time scale of channel gating (t_o and t_c). Such mechanisms can allow the modulation of $InsP_3R$ channel gating by the high local $[Ca^{2+}]_i$ at the inhibitory sites established during a channel opening to extend beyond the termination of that opening and the subsequent rapid collapse of the local $[Ca^{2+}]_i$ rise.

At the other extreme, with the gating of the channel completely decoupled from the fluctuations of local $[Ca^{2+}]_i$ caused by the openings and closings of the channel, the channel should gate with kinetics similar to those associated with one of the inhibitory sites exposed to a steady local $[Ca^{2+}]_i$ equivalent to that generated by a Ca^{2+} current of magnitude $P_o i_{Ca}$ passing through the pore, the same as the situation for the activating site. For realistic partial coupling between the two extremes, the inhibitory sites are effectively exposed to a time-averaged local $[Ca^{2+}]_i$ caused by a Ca^{2+} current of magnitude between $P_o i_{Ca}$ and i_{Ca}.

In summary, the observed sustained activation and inhibition of gating by Ca^{2+} flux through an $InsP_3R$ channel indicate that channel gating is not deterministically regulated by $[Ca^{2+}]_i$, and that a channel can respond to the Ca^{2+} flux through itself because its activation and inhibition kinetics enable it to sense an effective steady-state local flux-driven $[Ca^{2+}]_i$.

Estimates of the locations of functional cytoplasmic Ca^{2+}-binding sites from Ca^{2+} flux–mediated modulation of $InsP_3R$ channel activity

Our experiments demonstrate that $[Ca^{2+}]_{ER}$ modulates the activity of r-$InsP_3R$-3 channels in DT40-KO-r-$InsP_3R$-3 cells solely via the Ca^{2+} flux it drives through the channel that raises the local $[Ca^{2+}]_i$ at the cytoplasmic regulatory Ca^{2+}-binding sites. Using the steady-state $[Ca^{2+}]_i$ dependence of the channel P_o (Fig. 1), the effects of $[Ca^{2+}]_{ER}$ on channel activity can provide estimates of the effective time-averaged local $[Ca^{2+}]_i$ at the cytoplasmic activating or inhibitory Ca^{2+}-binding sites of the channel (Table 1). $[Ca^{2+}]_i$ profiles ($[Ca^{2+}]_i$ at various distances from the channel pore) were numerically generated (Materials and methods) for the different Ca^{2+}-buffering conditions, Ca^{2+} electrochemical gradients, and cytoplasmic ligand concentrations used in our experiments (Table 1). Checking the estimates of the effective time-averaged local $[Ca^{2+}]_i$ at the regulatory sites against the appropriate simulated $[Ca^{2+}]_i$ profiles, estimates can be made of the locations of the regulatory Ca^{2+}-binding sites relative to the channel pore, which is situated at the center of the channel based on the structural symmetry of the tetrameric $InsP_3R$ channel (Foskett et al., 2007).

For the inhibitory Ca^{2+} sites, depending on the degree of coupling between the gating of the channel and the fluctuations in local $[Ca^{2+}]_i$ associated with each opening and closing event, the $[Ca^{2+}]_i$ profile suitable for estimating the location of the sites lies between the $[Ca^{2+}]_i$ profile generated for Ca^{2+} current = i_{Ca} derived from the Goldman–Hodgkin–Katz current equation (Eq. 1) (for deterministic coupling between channel gating and the local $[Ca^{2+}]_i$ at the inhibitory Ca^{2+} site), and the profile generated for Ca^{2+} current = $P_o i_{Ca}$ (for completely uncoupled channel gating and local $[Ca^{2+}]_i$ at the inhibitory site). Because the exact degree of coupling between channel gating and local $[Ca^{2+}]_i$ fluctuations for the experimental conditions used are not known, we use the two $[Ca^{2+}]_i$ profiles for currents = i_{Ca} and $P_o i_{Ca}$ to derive upper and lower limits for the distance of the inhibitory Ca^{2+} sites from the channel pore.

In this study, we made six independent measurements of the inhibitory effects on channel gating of raising local $[Ca^{2+}]_i$ around the r-$InsP_3R$-3 channel beyond 2 μM (optimal $[Ca^{2+}]_i$) (shown in Figs. 2, A and C, 3 A, 6, A and B, and 8 A), each of which provides an independent estimate of the range for the distance of the inhibitory Ca^{2+}-binding site from the channel pore (Fig. 11, A–F, and Table 1). The estimated upper limits of this distance range between 21 and 44 nm (Table 1), with an average of 34 ± 4 nm. The estimated lower limits range between 2 and 29 nm (Table 1), with an average of 19 ± 4 nm. These suggest that the distance from the channel pore to the inhibitory site is ∼20–30 nm.

Using image reconstructions based on electron cryomicroscopy or electron microscopy with negative staining, 3-D structures of single tetrameric $InsP_3R$ channel have been determined (Jiang et al., 2002; da Fonseca et al., 2003; Hamada et al., 2003; Serysheva et al., 2003;

Sato et al., 2004; Wolfram et al., 2010; Ludtke et al., 2011). Although the details differ significantly, they generally show a large structure on the cytoplasmic side with maximum radius (r) from the channel pore axis between 10.5 and 14.2 nm, and height above the ER membrane (h) between 13.5 and 18.3 nm. Simple geometric consideration for a 3-D structure suggests that the maximum distance between the channel pore and a Ca^{2+}-binding site on the channel is ~24–32.5 nm ($r+h$). Thus, our estimate of the inhibitory site being 20–30 nm from the pore of the channel is not in conflict with the 3-D structures reported and suggests that the inhibitory site may be located in a part of the channel furthest from the pore.

For the activating Ca^{2+} sites, an upper limit for the distance to the channel pore can be derived from the $[Ca^{2+}]_i$ profile for current with magnitude = $P_o\, i_{Ca}$, which corresponds to the extreme case when the channel gating is completely decoupled from local $[Ca^{2+}]_i$ at the activating sites during channel openings and closings. However, no lower limit can be deduced for the pore-to-activating-site distance from the extreme case with channel gating rigidly dictated by local $[Ca^{2+}]_i$ at the activating sites. This is because in this case, the channel cannot be activated by $[Ca^{2+}]_{ER}$-driven Ca^{2+} flux through the pore, no matter where the activating Ca^{2+} sites are.

We made five independent measurements of the activating effects on channel gating of raising local $[Ca^{2+}]_i$ around the channel above 70 nM (resting $[Ca^{2+}]_i$) (Figs. 4 A, 5 A, and 9, A–C). These provided five independent estimates of the upper limits for the activating site to channel pore distance (Fig. 11, G–K, and Table 1), suggesting that the activating site is less than ~9–62 nm from the channel pore, which is also consistent with the 3-D structures of the channel. Moreover, 5 mM diBrBAPTA can effectively buffer the local $[Ca^{2+}]_i$ at the inhibitory Ca^{2+}-binding sites to abolish the inhibiting effect of Ca^{2+} flux driven through the channel by 1.1 mM $[Ca^{2+}]_{ER}$ at V_{app} = +30 mV (Fig. 8 A), whereas even 10 mM BAPTA cannot sufficiently buffer the local $[Ca^{2+}]_i$ at the activating Ca^{2+}-binding sites to abolish the activating effect of Ca^{2+} flux driven by 0.55 mM $[Ca^{2+}]_{ER}$ at the same V_{app} (Fig. 9 A). These observations strongly suggest that the activating Ca^{2+} sites are closer to the channel pore than the inhibitory sites.

It should be pointed out that these estimates of the locations of the cytoplasmic regulatory Ca^{2+} sites relative to the channel pore are very rough because the $[Ca^{2+}]_i$ profiles around the channel were simulated without taking into consideration factors that can affect the distribution of Ca^{2+} around the channel but are not known in any detail, like the 3-D surface topology and charge distribution of the channel.

A very similar approach to that used here was applied to estimate the locations of activating and inhibitory Ca^{2+}-binding sites in the RyR intracellular Ca^{2+} release channel that also exhibits $[Ca^{2+}]_{ER}$-driven Ca^{2+} flux modulation of channel activity (Liu et al., 2010). However, in that study, the couplings between channel gating and the local $[Ca^{2+}]_i$ fluctuations at the regulatory sites during channel openings and closings were not taken into consideration. The distances derived from the effective time-averaged $[Ca^{2+}]_i$ profile generated from Ca^{2+} current of magnitude = $P_o\, i_{Ca}$ was assumed to be estimates of the actual distances between the regulatory sites and the channel pore, instead of limiting values of those distances. This led to their conclusion that the inhibitory Ca^{2+} site was

TABLE 1

Estimations of the distances between cytoplasmic regulatory Ca^{2+}-binding sites and the channel pore axis

Representative current trace	Experimental conditions					Mean P_o	i_{Ca}	$i_{Ca}\, P_o$	$[Ca^{2+}]_i$ profiles	Regulatory Ca^{2+} site	$[Ca^{2+}]_i$ at site	Range of distance from pore
	$[InsP_3]$	$[Ca^{2+}]_{ER}$[a]	Bulk $[Ca^{2+}]_i$[b]	V_{app}	Cytoplasmic Ca^{2+} buffering							
	μM			*mV*			*fA*	*fA*			*μM*	*nm*
Fig. 2 (A and B)	3	300 μM	2 μM	−30	0.5 mM diBrBAPTA	0.22	230	51	Fig. 11 A	Inhibitory	5.7 μM	$12 < x < 39$
Fig. 2 C	10	300 μM	2 μM	−30	0.5 mM diBrBAPTA	0.7	230	161	Fig. 11 B	Inhibitory	7.2 μM	$23 < x < 31$
Fig. 3 A	10	1.1 mM	2 μM	−30	0.5 mM diBrBAPTA	0.46	830	380	Fig. 11 C	Inhibitory	14.3 μM	$25 < x < 42$
Fig. 6 A	3	300 μM	2 μM	−30	0.1 mM HEDTA	0.09	230	21	Fig. 11 D	Inhibitory	12 μM	$2 < x < 21$
Fig. 6 B	3	300 μM	2 μM	−30	5 mM diBrBAPTA	0.4	230	92	Fig. 11 E	Inhibitory	3.1 μM	$29 < x < 44$
Fig. 8 A	10	1.1 mM	2 μM	+30	5 mM diBrBAPTA	0.7	75	53	Fig. 11 F	Inhibitory	3.1 μM	$22 < x < 27$
Fig. 4 A	10	300 μM	55 nM	−30	0.5 mM BAPTA	0.29	230	64	Fig. 11 G	Activating	500 nM	$x < 62$
Fig. 5 A	10	300 μM	55 nM	+30	0.5 mM BAPTA	0.12	20	2.5	Fig. 11 H	Activating	150 nM	$x < 22$
Fig. 9 A	10	550 μM	55 nM	+30	10 mM BAPTA	0.25	38	10	Fig. 11 I	Activating	410 nM	$x < 13$
Fig. 9 B	10	550 μM	55 nM	+50	10 mM BAPTA	0.08	12	1	Fig. 11 J	Activating	100 nM	$x < 14$
Fig. 9 C	10	550 μM	55 nM	+70	10 mM BAPTA	0.05	3	0.15	Fig. 11 K	Activating	80 nM	$x < 9$

[a]$[Ca^{2+}]_{ER}$ = free $[Ca^{2+}]$ in perfusion solution.

[b]Bulk $[Ca^{2+}]_i$ = $[Ca^{2+}]_i$ at large distance from the channel pore = $[Ca^{2+}]_{r\to\infty}$ = free $[Ca^{2+}]$ in pipette solution.

1.2 ± 0.16 nm from the channel pore. This is probably an underestimation because that was actually the lower limit of the distance. The activating Ca^{2+} site to channel pore distance was calculated to be 1.7 µm, which led to a conclusion that the activating site on the open channel was shielded from the channel's own Ca^{2+} flux. However, this value should be the upper limit of the activating Ca^{2+} site to pore distance. Accordingly, their derivation does not provide strong support for the notion that the activating site is shielded from feed-through effects of the channel's own Ca^{2+} flux.

Limitation of the excised lum-out nuclear patch-clamp experiments

Using excised-patch lum-out nuclear patch clamping, we have demonstrated that all modulation by $[Ca^{2+}]_{ER}$ of the gating activity of the r-$InsP_3R$-3 channel can be attributed to feed-through effects causing a rise in local $[Ca^{2+}]_i$ at cytoplasmic regulatory Ca^{2+}-binding sites of the channel. We found no modulatory effects on $InsP_3R$ channel gating involving luminal Ca^{2+}-binding site(s) on the channel. However, it must be noted that the luminal side of the excised nuclear membrane patches was perfused

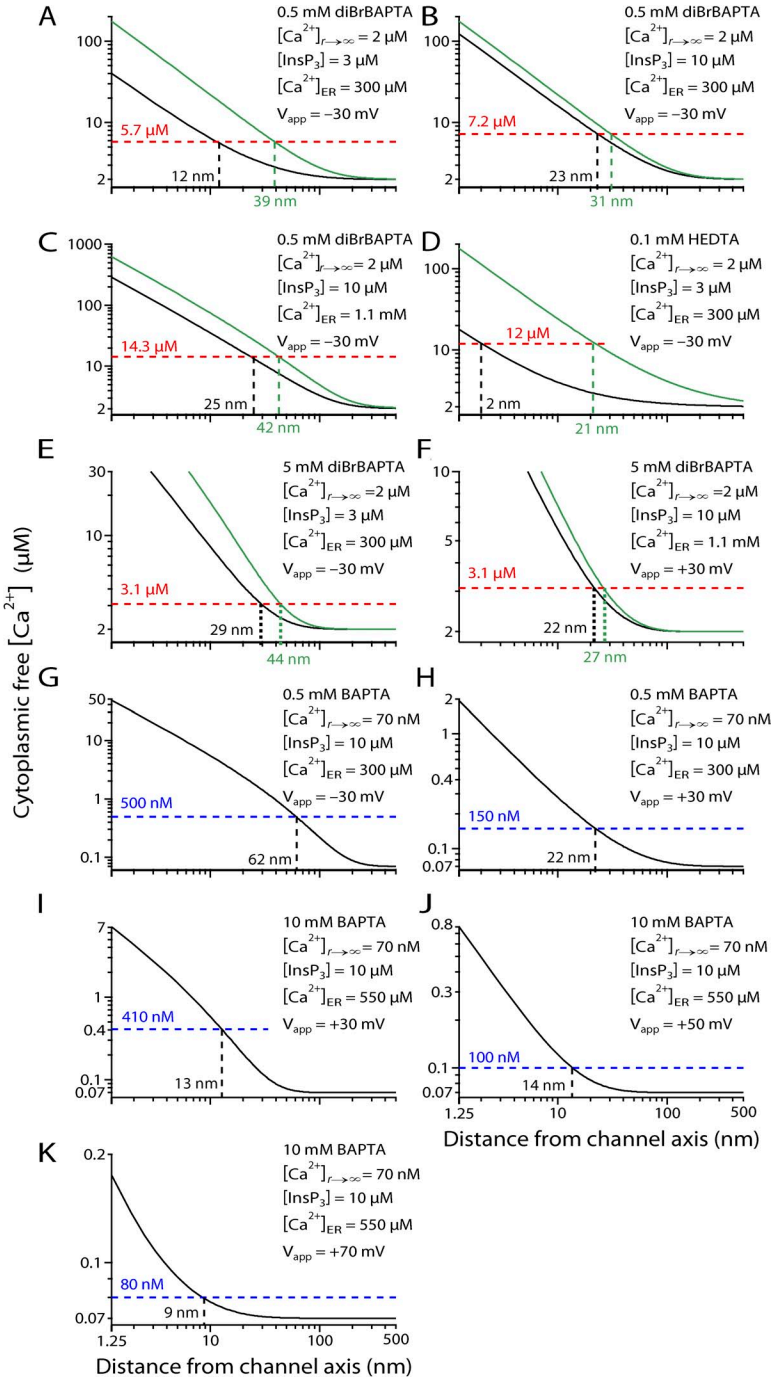

Figure 11. Estimated effective time-averaged $[Ca^{2+}]_i$ determining $InsP_3R$ channel gating activity, as sensed by cytoplasmic regulatory Ca^{2+}-binding sites at various distances from the channel pore in various lum-out experiments. Pipette solution $[Ca^{2+}]_f$ ($[Ca^{2+}]_{r\to\infty}$), perfusion solution $[Ca^{2+}]_f$ ($[Ca^{2+}]_{ER}$), V_{app}, $[InsP_3]$, and cytoplasmic Ca^{2+}-buffering conditions used in each set of experiment are tabulated in each corresponding graph. A–F are related to experiments investigating the effect of Ca^{2+} flux mediated by the cytoplasmic inhibitory Ca^{2+}-binding site(s), whereas G–K are related to experiments investigating the effect mediated by the cytoplasmic activating site(s). The effective $[Ca^{2+}]_i$ that produced the observed channel P_o are marked by dotted lines and tabulated (in red for inhibitory Ca^{2+} site and in blue for activating Ca^{2+} site). Black curves are effective $[Ca^{2+}]_i$ profiles derived from Ca^{2+} flux of magnitude = $P_o\, i_{Ca}$. The limits for the distances between the regulatory Ca^{2+}-binding site and the channel pore derived from these $[Ca^{2+}]_i$ profiles are marked by black dotted lines and tabulated in black. Green curves in A–F are effective $[Ca^{2+}]_i$ profiles derived from Ca^{2+} flux of magnitude = i_{Ca}. The upper limits for the distances between the inhibitory Ca^{2+} site to the channel pore derived from these $[Ca^{2+}]_i$ profiles are marked by green dotted lines and tabulated in green.

with various solutions to change $[Ca^{2+}]_{ER}$ in our experiments. It is possible that a luminal Ca^{2+}-binding factor(s) that could mediate effects of $[Ca^{2+}]_{ER}$ on $InsP_3R$ channel activity was washed off by the perfusion. The possible existence of $[Ca^{2+}]_{ER}$ regulation of $InsP_3R$ channel activity mediated by factor(s) in the ER lumen loosely associated with the channel should be investigated in the future using nuclear patch-clamp experiments in which the ER luminal milieu is preserved.

This work was supported by National Institutes of Health grants R01 MH059937 (to J.K. Foskett) and 5R01 GM065830 (to J.E. Pearson, D.-O.D. Mak, and J.K. Foskett).

Sharona E. Gordon served as editor.

Submitted: 21 March 2012
Accepted: 23 October 2012

REFERENCES

Beecroft, M.D., and C.W. Taylor. 1997. Incremental Ca^{2+} mobilization by inositol trisphosphate receptors is unlikely to be mediated by their desensitization or regulation by luminal or cytosolic Ca^{2+}. *Biochem. J.* 326:215–220.

Berridge, M.J. 1993. Inositol trisphosphate and calcium signalling. *Nature.* 361:315–325. http://dx.doi.org/10.1038/361315a0

Berridge, M.J. 1997. Elementary and global aspects of calcium signalling. *J. Physiol.* 499:291–306.

Berridge, M.J. 1998. Neuronal calcium signaling. *Neuron.* 21:13–26. http://dx.doi.org/10.1016/S0896-6273(00)80510-3

Berridge, M.J. 2003. Cardiac calcium signalling. *Biochem. Soc. Trans.* 31:930–933. http://dx.doi.org/10.1042/BST0310930

Berridge, M.J., P. Lipp, and M.D. Bootman. 2000. The versatility and universality of calcium signalling. *Nat. Rev. Mol. Cell Biol.* 1:11–21. http://dx.doi.org/10.1038/35036035

Bers, D.M., C.W. Patton, and R. Nuccitelli. 2010. A practical guide to the preparation of Ca^{2+} buffers. *Methods Cell Biol.* 99:1–26. http://dx.doi.org/10.1016/B978-0-12-374841-6.00001-3

Betzenhauser, M.J., L.E. Wagner II, M. Iwai, T. Michikawa, K. Mikoshiba, and D.I. Yule. 2008. ATP modulation of Ca^{2+} release by type-2 and type-3 inositol (1, 4, 5)-triphosphate receptors. Differing ATP sensitivities and molecular determinants of action. *J. Biol. Chem.* 283:21579–21587. http://dx.doi.org/10.1074/jbc.M801680200

Bezprozvanny, I., and B.E. Ehrlich. 1994. Inositol (1,4,5)-trisphosphate ($InsP_3$)-gated Ca channels from cerebellum: conduction properties for divalent cations and regulation by intraluminal calcium. *J. Gen. Physiol.* 104:821–856. http://dx.doi.org/10.1085/jgp.104.5.821

Bezprozvanny, I., and B.E. Ehrlich. 1995. The inositol 1,4,5-trisphosphate ($InsP_3$) receptor. *J. Membr. Biol.* 145:205–216.

Bootman, M. 1994a. Intracellular calcium. Questions about quantal Ca^{2+} release. *Curr. Biol.* 4:169–172. http://dx.doi.org/10.1016/S0960-9822(94)00041-2

Bootman, M.D. 1994b. Quantal Ca^{2+} release from $InsP_3$-sensitive intracellular Ca^{2+} stores. *Mol. Cell. Endocrinol.* 98:157–166. http://dx.doi.org/10.1016/0303-7207(94)90134-1

Bootman, M.D., T.J. Collins, C.M. Peppiatt, L.S. Prothero, L. MacKenzie, P. De Smet, M. Travers, S.C. Tovey, J.T. Seo, M.J. Berridge, et al. 2001. Calcium signalling—an overview. *Semin. Cell Dev. Biol.* 12:3–10. http://dx.doi.org/10.1006/scdb.2000.0211

Braet, K., L. Cabooter, K. Paemeleire, and L. Leybaert. 2004. Calcium signal communication in the central nervous system. *Biol. Cell.* 96:79–91. http://dx.doi.org/10.1016/j.biolcel.2003.10.007

Butler, J.N. 1968. The thermodynamic activity of calcium ion in sodium chloride-calcium chloride electrolytes. *Biophys. J.* 8:1426–1433. http://dx.doi.org/10.1016/S0006-3495(68)86564-6

Button, D., and A. Eidsath. 1996. Aequorin targeted to the endoplasmic reticulum reveals heterogeneity in luminal Ca^{++} concentration and reports agonist- or IP_3-induced release of Ca^{++}. *Mol. Biol. Cell.* 7:419–434.

Bygrave, F.L., and A. Benedetti. 1996. What is the concentration of calcium ions in the endoplasmic reticulum? *Cell Calcium.* 19:547–551. http://dx.doi.org/10.1016/S0143-4160(96)90064-0

Cárdenas, C., R.A. Miller, I. Smith, T. Bui, J. Molgó, M. Müller, H. Vais, K.H. Cheung, J. Yang, I. Parker, et al. 2010. Essential regulation of cell bioenergetics by constitutive $InsP_3$ receptor Ca^{2+} transfer to mitochondria. *Cell.* 142:270–283. http://dx.doi.org/10.1016/j.cell.2010.06.007

Caroppo, R., M. Colella, A. Colasuonno, A. DeLuisi, L. Debellis, S. Curci, and A.M. Hofer. 2003. A reassessment of the effects of luminal $[Ca^{2+}]$ on inositol 1,4,5-trisphosphate-induced Ca^{2+} release from internal stores. *J. Biol. Chem.* 278:39503–39508. http://dx.doi.org/10.1074/jbc.M305823200

Cheung, K.H., D. Shineman, M. Müller, C. Cárdenas, L. Mei, J. Yang, T. Tomita, T. Iwatsubo, V.M. Lee, and J.K. Foskett. 2008. Mechanism of Ca^{2+} disruption in Alzheimer's disease by presenilin regulation of $InsP_3$ receptor channel gating. *Neuron.* 58:871–883. http://dx.doi.org/10.1016/j.neuron.2008.04.015

Clapham, D.E. 1995. Calcium signaling. *Cell.* 80:259–268. http://dx.doi.org/10.1016/0092-8674(95)90408-5

Combettes, L., M. Claret, and P. Champeil. 1992. Do submaximal $InsP_3$ concentrations only induce the partial discharge of permeabilized hepatocyte calcium pools because of the concomitant reduction of intraluminal Ca^{2+} concentration? *FEBS Lett.* 301:287–290. http://dx.doi.org/10.1016/0014-5793(92)80258-I

Combettes, L., T.R. Cheek, and C.W. Taylor. 1996. Regulation of inositol trisphosphate receptors by luminal Ca^{2+} contributes to quantal Ca^{2+} mobilization. *EMBO J.* 15:2086–2093.

Cussler, E.L. 1997. Diffusion: Mass Transfer in Fluid Systems. Second edition. Cambridge University Press, Cambridge. 580 pp.

da Fonseca, P.C., S.A. Morris, E.P. Nerou, C.W. Taylor, and E.P. Morris. 2003. Domain organization of the type 1 inositol 1,4,5-trisphosphate receptor as revealed by single-particle analysis. *Proc. Natl. Acad. Sci. USA.* 100:3936–3941. http://dx.doi.org/10.1073/pnas.0536251100

Dawson, A.P., E.J. Lea, and R.F. Irvine. 2003. Kinetic model of the inositol trisphosphate receptor that shows both steady-state and quantal patterns of Ca^{2+} release from intracellular stores. *Biochem. J.* 370:621–629. http://dx.doi.org/10.1042/BJ20021289

Dupont, G., and S. Swillens. 1996. Quantal release, incremental detection, and long-period Ca^{2+} oscillations in a model based on regulatory Ca^{2+}-binding sites along the permeation pathway. *Biophys. J.* 71:1714–1722. http://dx.doi.org/10.1016/S0006-3495(96)79373-6

Ferris, C.D., A.M. Cameron, R.L. Huganir, and S.H. Snyder. 1992. Quantal calcium release by purified reconstituted inositol 1,4,5-trisphosphate receptors. *Nature.* 356:350–352. http://dx.doi.org/10.1038/356350a0

Foskett, J.K. 2010. Inositol trisphosphate receptor Ca^{2+} release channels in neurological diseases. *Pflugers Arch.* 460:481–494. http://dx.doi.org/10.1007/s00424-010-0826-0

Foskett, J.K., C. White, K.H. Cheung, and D.-O.D. Mak. 2007. Inositol trisphosphate receptor Ca^{2+} release channels. *Physiol. Rev.* 87:593–658. http://dx.doi.org/10.1152/physrev.00035.2006

Fraiman, D., and S.P. Dawson. 2004. A model of IP_3 receptor with a luminal calcium binding site: stochastic simulations and analysis. *Cell Calcium.* 35:403–413. http://dx.doi.org/10.1016/j.ceca.2003.10.004

Furuichi, T., and K. Mikoshiba. 1995. Inositol 1, 4, 5-trisphosphate receptor-mediated Ca^{2+} signaling in the brain. *J. Neurochem.* 64:953–960. http://dx.doi.org/10.1046/j.1471-4159.1995.64030953.x

Hagar, R.E., and B.E. Ehrlich. 2000. Regulation of the type III $InsP_3$ receptor and its role in β cell function. *Cell. Mol. Life Sci.* 57:1938–1949. http://dx.doi.org/10.1007/PL00000674

Hamada, K., A. Terauchi, and K. Mikoshiba. 2003. Three-dimensional rearrangements within inositol 1,4,5-trisphosphate receptor by calcium. *J. Biol. Chem.* 278:52881–52889. http://dx.doi.org/10.1074/jbc.M309743200

Higo, T., M. Hattori, T. Nakamura, T. Natsume, T. Michikawa, and K. Mikoshiba. 2005. Subtype-specific and ER lumenal environment-dependent regulation of inositol 1,4,5-trisphosphate receptor type 1 by ERp44. *Cell.* 120:85–98. http://dx.doi.org/10.1016/j.cell.2004.11.048

Hille, B. 2001. Ionic Channels of Excitable Membranes. Third edition. Sinauer Associates, Inc., Sunderland, MA. 814 pp.

Ionescu, L., K.H. Cheung, H. Vais, D.-O.D. Mak, C. White, and J.K. Foskett. 2006. Graded recruitment and inactivation of single $InsP_3$ receptor Ca^{2+}-release channels: implications for quantal Ca^{2+} release. *J. Physiol.* 573:645–662. http://dx.doi.org/10.1113/jphysiol.2006.109504

Irvine, R.F. 1990. 'Quantal' Ca^{2+} release and the control of Ca^{2+} entry by inositol phosphates—a possible mechanism. *FEBS Lett.* 263:5–9. http://dx.doi.org/10.1016/0014-5793(90)80692-C

Jiang, Q.X., E.C. Thrower, D.W. Chester, B.E. Ehrlich, and F.J. Sigworth. 2002. Three-dimensional structure of the type 1 inositol 1,4,5-trisphosphate receptor at 24 Å resolution. *EMBO J.* 21:3575–3581. http://dx.doi.org/10.1093/emboj/cdf380

Johenning, F.W., and B.E. Ehrlich. 2002. Signaling microdomains: $InsP_3$ receptor localization takes on new meaning. *Neuron.* 34:173–175. http://dx.doi.org/10.1016/S0896-6273(02)00665-7

Joseph, S.K. 1996. The inositol triphosphate receptor family. *Cell. Signal.* 8:1–7. http://dx.doi.org/10.1016/0898-6568(95)02012-8

Joseph, S.K., and G. Hajnóczky. 2007. IP_3 receptors in cell survival and apoptosis: Ca^{2+} release and beyond. *Apoptosis.* 12:951–968. http://dx.doi.org/10.1007/s10495-007-0719-7

Kang, S., J. Kang, H. Kwon, D. Frueh, S.H. Yoo, G. Wagner, and S. Park. 2008. Effects of redox potential and Ca^{2+} on the inositol 1,4,5-trisphosphate receptor L3-1 loop region: implications for receptor regulation. *J. Biol. Chem.* 283:25567–25575. http://dx.doi.org/10.1074/jbc.M803321200

Kindman, L.A., and T. Meyer. 1993. Use of intracellular Ca^{2+} stores from rat basophilic leukemia cells to study the molecular mechanism leading to quantal Ca^{2+} release by inositol 1,4,5-trisphosphate. *Biochemistry.* 32:1270–1277. http://dx.doi.org/10.1021/bi00056a011

Laver, D.R. 2007a. Ca^{2+} stores regulate ryanodine receptor Ca^{2+} release channels via luminal and cytosolic Ca^{2+} sites. *Biophys. J.* 92:3541–3555. http://dx.doi.org/10.1529/biophysj.106.099028

Laver, D.R. 2007b. Ca^{2+} stores regulate ryanodine receptor Ca^{2+} release channels via luminal and cytosolic Ca^{2+} sites. *Clin. Exp. Pharmacol. Physiol.* 34:889–896. http://dx.doi.org/10.1111/j.1440-1681.2007.04708.x

Lewis, C.A. 1979. Ion-concentration dependence of the reversal potential and the single channel conductance of ion channels at the frog neuromuscular junction. *J. Physiol.* 286:417–445.

Li, G., M. Mongillo, K.T. Chin, H. Harding, D. Ron, A.R. Marks, and I. Tabas. 2009. Role of ERO1-α–mediated stimulation of inositol 1,4,5-triphosphate receptor activity in endoplasmic reticulum stress–induced apoptosis. *J. Cell Biol.* 186:783–792. http://dx.doi.org/10.1083/jcb.200904060

Liu, Y., M. Porta, J. Qin, J. Ramos, A. Nani, T.R. Shannon, and M. Fill. 2010. Flux regulation of cardiac ryanodine receptor channels. *J. Gen. Physiol.* 135:15–27. http://dx.doi.org/10.1085/jgp.200910273

Ludtke, S.J., T.P. Tran, Q.T. Ngo, V.Y. Moiseenkova-Bell, W. Chiu, and I.I. Serysheva. 2011. Flexible architecture of IP_3R1 by Cryo-EM. *Structure.* 19:1192–1199. http://dx.doi.org/10.1016/j.str.2011.05.003

MacKrill, J.J. 1999. Protein-protein interactions in intracellular Ca^{2+}-release channel function. *Biochem. J.* 337:345–361. http://dx.doi.org/10.1042/0264-6021:3370345

Mak, D.-O.D., and J.K. Foskett. 1998. Effects of divalent cations on single-channel conduction properties of *Xenopus* IP_3 receptor. *Am. J. Physiol.* 275:C179–C188.

Mak, D.-O.D., S. McBride, and J.K. Foskett. 1998. Inositol 1,4,5-trisphosphate activation of inositol trisphosphate receptor Ca^{2+} channel by ligand tuning of Ca^{2+} inhibition. *Proc. Natl. Acad. Sci. USA.* 95:15821–15825. http://dx.doi.org/10.1073/pnas.95.26.15821

Mak, D.-O.D., S. McBride, and J.K. Foskett. 1999. ATP regulation of type 1 inositol 1,4,5-trisphosphate receptor channel gating by allosteric tuning of Ca^{2+} activation. *J. Biol. Chem.* 274:22231–22237. http://dx.doi.org/10.1074/jbc.274.32.22231

Mak, D.-O.D., S. McBride, and J.K. Foskett. 2001a. ATP-dependent adenophostin activation of inositol 1,4,5-trisphosphate receptor channel gating: kinetic implications for the durations of calcium puffs in cells. *J. Gen. Physiol.* 117:299–314. http://dx.doi.org/10.1085/jgp.117.4.299

Mak, D.-O.D., S. McBride, and J.K. Foskett. 2001b. Regulation by Ca^{2+} and inositol 1,4,5-trisphosphate ($InsP_3$) of single recombinant type 3 $InsP_3$ receptor channels. Ca^{2+} activation uniquely distinguishes types 1 and 3 $Insp_3$ receptors. *J. Gen. Physiol.* 117:435–446. http://dx.doi.org/10.1085/jgp.117.5.435

Mak, D.-O.D., S.M. McBride, and J.K. Foskett. 2003. Spontaneous channel activity of the inositol 1,4,5-trisphosphate ($InsP_3$) receptor ($InsP_3R$). Application of allosteric modeling to calcium and $InsP_3$ regulation of $InsP_3R$ single-channel gating. *J. Gen. Physiol.* 122:583–603. http://dx.doi.org/10.1085/jgp.200308809

Mak, D.-O.D., C. White, L. Ionescu, and J.K. Foskett. 2005. Nuclear patch clamp electrophysiology of inositol trisphosphate receptor Ca^{2+} release channels. *In* Calcium Signaling. Second edition. J.W. Putney, Jr., editor. CRC Press, Boca Raton, FL. 203–229.

Mak, D.-O.D., J.E. Pearson, K.P.C. Loong, S. Datta, M. Fernández-Mongil, and J.K. Foskett. 2007. Rapid ligand-regulated gating kinetics of single inositol 1,4,5-trisphosphate receptor Ca^{2+} release channels. *EMBO Rep.* 8:1044–1051. http://dx.doi.org/10.1038/sj.embor.7401087

Marks, A.R. 1997. Intracellular calcium-release channels: regulators of cell life and death. *Am. J. Physiol.* 272:H597–H605.

McCarron, J.G., S. Chalmers, and T.C. Muir. 2008. "Quantal" Ca^{2+} release at the cytoplasmic aspect of the $Ins(1,4,5)P_3R$ channel in smooth muscle. *J. Cell Sci.* 121:86–98. http://dx.doi.org/10.1242/jcs.017541

Meldolesi, J., and T. Pozzan. 1998. The endoplasmic reticulum Ca^{2+} store: a view from the lumen. *Trends Biochem. Sci.* 23:10–14. http://dx.doi.org/10.1016/S0968-0004(97)01143-2

Missiaen, L., H. De Smedt, G. Droogmans, and R. Casteels. 1992a. Ca^{2+} release induced by inositol 1,4,5-trisphosphate is a steady-state phenomenon controlled by luminal Ca^{2+} in permeabilized cells. *Nature.* 357:599–602. http://dx.doi.org/10.1038/357599a0

Missiaen, L., H. De Smedt, G. Droogmans, and R. Casteels. 1992b. Luminal Ca^{2+} controls the activation of the inositol 1,4,5-trisphosphate receptor by cytosolic Ca^{2+}. *J. Biol. Chem.* 267:22961–22966.

Missiaen, L., C.W. Taylor, and M.J. Berridge. 1992c. Luminal Ca^{2+} promoting spontaneous Ca^{2+} release from inositol trisphosphate-sensitive stores in rat hepatocytes. *J. Physiol.* 455:623–640.

Missiaen, L., H. De Smedt, J.B. Parys, I. Sienaert, S. Vanlingen, and R. Casteels. 1996. Effects of luminal Ca^{2+} on inositol trisphosphate-induced Ca^{2+} release: facts or artifacts? *Cell Calcium.* 19:91–93. http://dx.doi.org/10.1016/S0143-4160(96)90016-0

Naraghi, M. 1997. T-jump study of calcium binding kinetics of calcium chelators. *Cell Calcium.* 22:255–268. http://dx.doi.org/10.1016/S0143-4160(97)90064-6

Naraghi, M., and E. Neher. 1997. Linearized buffered Ca^{2+} diffusion in microdomains and its implications for calculation of [Ca^{2+}] at the mouth of a calcium channel. *J. Neurosci.* 17:6961–6973.

Neher, E. 1986. Concentrations profiles of intracellular calcium in the presence of a diffusible chelator. *In* Experimental Brain Research. Volume 14: Calcium Electrogenesis and Neuronal Functioning. U. Heinemann, M. Klee, E. Neher, and W. Singer, editors. Springer, Heidelberg. 80–96.

Neher, E. 1998. Usefulness and limitations of linear approximations to the understanding of Ca^{++} signals. *Cell Calcium.* 24:345–357. http://dx.doi.org/10.1016/S0143-4160(98)90058-6

Nunn, D.L., and C.W. Taylor. 1991. Regulation of Ca^{2+} mobilization by Ins (1,4,5)P_3 and intraluminal Ca^{2+} in permeabilized hepatocytes. *Biochem. Soc. Trans.* 19:206S.

Nunn, D.L., and C.W. Taylor. 1992. Luminal Ca^{2+} increases the sensitivity of Ca^{2+} stores to inositol 1,4,5-trisphosphate. *Mol. Pharmacol.* 41:115–119.

Orrenius, S., B. Zhivotovsky, and P. Nicotera. 2003. Regulation of cell death: the calcium-apoptosis link. *Nat. Rev. Mol. Cell Biol.* 4:552–565. http://dx.doi.org/10.1038/nrm1150

Parys, J.B., L. Missiaen, H. De Smedt, and R. Casteels. 1993. Loading dependence of inositol 1,4,5-trisphosphate-induced Ca^{2+} release in the clonal cell line A7r5. Implications for the mechanism of quantal Ca^{2+} release. *J. Biol. Chem.* 268:25206–25212.

Parys, J.B., L. Missiaen, H.D. Smedt, I. Sienaert, and R. Casteels. 1996. Mechanisms responsible for quantal Ca^{2+} release from inositol trisphosphate-sensitive calcium stores. *Pflugers Arch.* 432:359–367. http://dx.doi.org/10.1007/s004240050145

Patel, S., S.K. Joseph, and A.P. Thomas. 1999. Molecular properties of inositol 1,4,5-trisphosphate receptors. *Cell Calcium.* 25:247–264. http://dx.doi.org/10.1054/ceca.1999.0021

Patterson, R.L., D. Boehning, and S.H. Snyder. 2004. Inositol 1,4,5-trisphosphate receptors as signal integrators. *Annu. Rev. Biochem.* 73:437–465. http://dx.doi.org/10.1146/annurev.biochem.73.071403.161303

Putney, J.W., Jr., and G.S. Bird. 1993. The inositol phosphate-calcium signaling system in nonexcitable cells. *Endocr. Rev.* 14:610–631.

Qin, F., A. Auerbach, and F. Sachs. 2000a. A direct optimization approach to hidden Markov modeling for single channel kinetics. *Biophys. J.* 79:1915–1927. http://dx.doi.org/10.1016/S0006-3495(00)76441-1

Qin, F., A. Auerbach, and F. Sachs. 2000b. Hidden Markov modeling for single channel kinetics with filtering and correlated noise. *Biophys. J.* 79:1928–1944. http://dx.doi.org/10.1016/S0006-3495(00)76442-3

Randriamampita, C., and A. Trautmann. 2004. Ca^{2+} signals and T lymphocytes; "New mechanisms and functions in Ca^{2+} signalling". *Biol. Cell.* 96:69–78. http://dx.doi.org/10.1016/j.biolcel.2003.10.008

Renard-Rooney, D.C., G. Hajnóczky, M.B. Seitz, T.G. Schneider, and A.P. Thomas. 1993. Imaging of inositol 1,4,5-trisphosphate-induced Ca^{2+} fluxes in single permeabilized hepatocytes. Demonstration of both quantal and nonquantal patterns of Ca^{2+} release. *J. Biol. Chem.* 268:23601–23610.

Sato, C., K. Hamada, T. Ogura, A. Miyazawa, K. Iwasaki, Y. Hiroaki, K. Tani, A. Terauchi, Y. Fujiyoshi, and K. Mikoshiba. 2004. Inositol 1,4,5-trisphosphate receptor contains multiple cavities and L-shaped ligand-binding domains. *J. Mol. Biol.* 336:155–164. http://dx.doi.org/10.1016/j.jmb.2003.11.024

Serysheva, I.I., D.J. Bare, S.J. Ludtke, C.S. Kettlun, W. Chiu, and G.A. Mignery. 2003. Structure of the type 1 inositol 1,4,5-trisphosphate receptor revealed by electron cryomicroscopy. *J. Biol. Chem.* 278:21319–21322. http://dx.doi.org/10.1074/jbc.C300148200

Short, A.D., M.G. Klein, M.F. Schneider, and D.L. Gill. 1993. Inositol 1,4,5-trisphosphate-mediated quantal Ca^{2+} release measured by high resolution imaging of Ca^{2+} within organelles. *J. Biol. Chem.* 268:25887–25893.

Shuttleworth, T.J. 1992. Ca^{2+} release from inositol trisphosphate-sensitive stores is not modulated by intraluminal Ca^{2+}. *J. Biol. Chem.* 267:3573–3576.

Shuttleworth, T.J. 1995. A re-evaluation of the apparent effects of luminal Ca^{2+} on inositol 1,4,5-trisphosphate-induced Ca^{2+} release. *Cell Calcium.* 17:393–398. http://dx.doi.org/10.1016/0143-4160(95)90085-3

Smith, G.D. 1996. Analytical steady-state solution to the rapid buffering approximation near an open Ca^{2+} channel. *Biophys. J.* 71:3064–3072. http://dx.doi.org/10.1016/S0006-3495(96)79500-0

Steenbergen, J.M., and F.S. Fay. 1996. The quantal nature of calcium release to caffeine in single smooth muscle cells results from activation of the sarcoplasmic reticulum Ca^{2+}-ATPase. *J. Biol. Chem.* 271:7398–7403. http://dx.doi.org/10.1074/jbc.271.13.7398

Sugawara, H., M. Kurosaki, M. Takata, and T. Kurosaki. 1997. Genetic evidence for involvement of type 1, type 2 and type 3 inositol 1,4,5-trisphosphate receptors in signal transduction through the B-cell antigen receptor. *EMBO J.* 16:3078–3088. http://dx.doi.org/10.1093/emboj/16.11.3078

Swillens, S. 1992. Dynamic control of inositol 1,4,5-trisphosphate-induced Ca^{2+} release: a theoretical explanation for the quantal release of Ca^{2+}. *Mol. Pharmacol.* 41:110–114.

Swillens, S., L. Combettes, and P. Champeil. 1994. Transient inositol 1,4,5-trisphosphate-induced Ca^{2+} release: a model based on regulatory Ca^{2+}-binding sites along the permeation pathway. *Proc. Natl. Acad. Sci. USA.* 91:10074–10078. http://dx.doi.org/10.1073/pnas.91.21.10074

Tanimura, A., and R.J. Turner. 1996. Calcium release in HSY cells conforms to a steady-state mechanism involving regulation of the inositol 1,4,5-trisphosphate receptor Ca^{2+} channel by luminal [Ca^{2+}]. *J. Cell Biol.* 132:607–616. http://dx.doi.org/10.1083/jcb.132.4.607

Tanimura, A., Y. Tojyo, and Y. Matsumoto. 1998. Imaging of quantal calcium release in the inositol 1,4,5-trisphosphate-sensitive organelles of permeabilized HSY cells. *Cell Struct. Funct.* 23:129–135. http://dx.doi.org/10.1247/csf.23.129

Taufiq-Ur-Rahman, A. Skupin, M. Falcke, and C.W. Taylor. 2009. Clustering of $InsP_3$ receptors by $InsP_3$ retunes their regulation by $InsP_3$ and Ca^{2+}. *Nature.* 458:655–659. http://dx.doi.org/10.1038/nature07763

Taylor, C.W., and A.J. Laude. 2002. IP_3 receptors and their regulation by calmodulin and cytosolic Ca^{2+}. *Cell Calcium.* 32:321–334. http://dx.doi.org/10.1016/S0143416002001859

Taylor, C.W., and A. Richardson. 1991. Structure and function of inositol trisphosphate receptors. *Pharmacol. Ther.* 51:97–137. http://dx.doi.org/10.1016/0163-7258(91)90043-L

Thrower, E.C., H. Mobasheri, S. Dargan, P. Marius, E.J.A. Lea, and A.P. Dawson. 2000. Interaction of luminal calcium and cytosolic ATP in the control of type 1 inositol (1,4,5)-trisphosphate receptor channels. *J. Biol. Chem.* 275:36049–36055. http://dx.doi.org/10.1074/jbc.M000970200

Thrower, E.C., R.E. Hagar, and B.E. Ehrlich. 2001. Regulation of Ins(1,4,5)P_3 receptor isoforms by endogenous modulators. *Trends Pharmacol. Sci.* 22:580–586. http://dx.doi.org/10.1016/S0165-6147(00)01809-5

Tregear, R.T., A.P. Dawson, and R.F. Irvine. 1991. Quantal release of Ca^{2+} from intracellular stores by $InsP_3$: tests of the concept of control of Ca^{2+} release by intraluminal Ca^{2+}. *Proc. Biol. Sci.* 243:263–268. http://dx.doi.org/10.1098/rspb.1991.0040

Tsien, R.Y. 1980. New calcium indicators and buffers with high selectivity against magnesium and protons: design, synthesis, and properties of prototype structures. *Biochemistry.* 19:2396–2404. http://dx.doi.org/10.1021/bi00552a018

Vais, H., J.K. Foskett, and D.-O.D. Mak. 2010a. Unitary Ca^{2+} current through recombinant type 3 $InsP_3$ receptor channels under physiological ionic conditions. *J. Gen. Physiol.* 136:687–700. http://dx.doi.org/10.1085/jgp.201010513

Vais, H., A.P. Siebert, Z. Ma, M. Fernández-Mongil, J.K. Foskett, and D.-O.D. Mak. 2010b. Redox-regulated heterogeneous thresholds for ligand recruitment among $InsP_3R$ Ca^{2+}-release channels. *Biophys. J.* 99:407–416. http://dx.doi.org/10.1016/j.bpj.2010.04.034

Vais, H., J.K. Foskett, and D.-O.D. Mak. 2011. $InsP_3R$ channel gating altered by clustering? *Nature.* 478:E1–E2. http://dx.doi.org/10.1038/nature10493

Wagner, L.E., II, S.K. Joseph, and D.I. Yule. 2008. Regulation of single inositol 1,4,5-trisphosphate receptor channel activity by protein kinase A phosphorylation. *J. Physiol.* 586:3577–3596. http://dx.doi.org/10.1113/jphysiol.2008.152314

Wolfram, F., E. Morris, and C.W. Taylor. 2010. Three-dimensional structure of recombinant type 1 inositol 1,4,5-trisphosphate receptor. *Biochem. J.* 428:483–489. http://dx.doi.org/10.1042/BJ20100143

Yamasaki-Mann, M., and I. Parker. 2011. Enhanced ER Ca^{2+} store filling by overexpression of SERCA2b promotes IP_3-evoked puffs. *Cell Calcium.* 50:36–41. http://dx.doi.org/10.1016/j.ceca.2011.04.008

Yu, R., and P.M. Hinkle. 2000. Rapid turnover of calcium in the endoplasmic reticulum during signaling. Studies with cameleon calcium indicators. *J. Biol. Chem.* 275:23648–23653. http://dx.doi.org/10.1074/jbc.M002684200